Dorsal Horn Circuits for Persistent Mechanical Pain

Cedric Peirs, Sean-Paul G Williams, Xinyi Zhao, Claire E Walsh, Jeremy Y Gedeon, Natalie E Cagle, Adam C Goldring, Hiroyuki Hioki, Zheng Liu, Paulina S Marell, et al.

Dorsal Horn Circuits for Persistent Mechanical Pain.

.

Cedric Peirs[1,2,5], Sean-Paul G. Williams[1,2,5], Xinyi Zhao[1,2,3], Claire E. Walsh[1], Jeremy Y. Gedeon[1], Natalie E. Cagle[1], Adam C. Goldring[1], Hiroyuki Hioki[4], Zheng Liu[1], Paulina S. Marell[1], and Rebecca P. Seal[1,2,*]

1. Departments of Neurobiology and Otolaryngology, University of Pittsburgh School of Medicine, 3501 Fifth Ave, BST3, Pittsburgh, Pennsylvania 15213, USA
2. Pittsburgh Center for Pain Research, University of Pittsburgh School of Medicine, 200 Lothrop St, Pittsburgh, Pennsylvania 15213, USA
3. Tsinghua M.D. Program, Tsinghua University School of Medicine, 30 Shuang Qing Lu, Haidian District, Beijing, 100084, China
4. Department of Morphological Brain Science, Graduate School of Medicine, Kyoto University, Kyoto 606-8501, Japan.
5. These authors contributed equally.

Running Title: Dorsal Horn Neurons Conveying Mechanical Hypersensitivity

Number of Text Pages: 41
Number of Figures: 8
Number of words in Summary: 146
Number of characters with spaces: 69,169
Supplemental material: 7 Figures and 2 Movies with Legends, Experimental Procedures and References
Conflicts of Interest: None to report

*Corresponding author: Rebecca Seal, University of Pittsburgh Department of Neurobiology, 6058 BST3, 3501 Fifth Avenue, Pittsburgh, PA 15213, rpseal@pitt.edu

SUMMARY

Persistent mechanical hypersensitivity that occurs in the setting of injury or disease remains a major clinical problem largely because the underlying neural circuitry is still not known. Here we report the functional identification of key components of the elusive dorsal horn circuit for mechanical allodynia. We show that the transient expression of VGLUT3 by a discrete population of neurons in the deep dorsal horn is required for mechanical pain and that activation of the cells in the adult conveys mechanical hypersensitivity. The cells, which receive direct low threshold input, point to a novel location for circuit initiation. Subsequent analysis of c-Fos reveals the circuit extends dorsally to nociceptive lamina I projection neurons, and includes lamina II calretinin neurons, which we show also convey mechanical allodynia. Lastly, using inflammatory and neuropathic pain models, we show that multiple microcircuits in the dorsal horn encode this form of pain.

INTRODUCTION

Mechanical pain conveyed acutely is beneficial, serving to warn the body of impending injury. However, persistent pain that results from injury or disease often becomes pathological, debilitating and is difficult to treat (Varrassi et al., 2010). Persistent pain states typically manifest as an increased sensitivity to thermal or mechanical stimuli. The latter allodynic state, in which innocuous touch or movement is perceived as painful, is one of the most clinically problematic forms of pain.

Persistent pain conditions are typically initiated by the dysregulation of primary sensory neurons leading to central sensitization within the spinal cord network and brain (Kuner, 2010; Prescott et al., 2014; von Hehn et al., 2012). The spinal cord dorsal horn is a major site of integration for somatosensory information and is composed of numerous excitatory and inhibitory interneuron populations and a relatively small number of output neurons (Todd, 2010). Information processing in this structure is crudely segregated, such that primary afferents conveying thermal and nociceptive information mainly innervate the superficial laminae, whereas those transmitting low threshold mechanical information generally target deeper laminae. Almost all output neurons are located in laminae I and III-V. The vast majority of lamina I projection neurons respond to noxious stimuli and express the receptor for neurokinin I (NK1R). These cells are thought to convey discriminative aspects of pain, such as the location and quality, as well as emotional aspects (Miraucourt et al., 2007; Todd, 2010). In the deep dorsal horn, most projection neurons are wide-dynamic range. These neurons respond to many different types of stimuli, possess very large receptive fields and code for stimulus intensity among other features (Craig, 2003).

One model proposed for the circuit level mechanisms underlying mechanical allodynia is based on the gate control theory, in which touch normally inhibits acute pain through direct activation of inhibitory interneurons (Melzack and Wall, 1965). Upon injury, however, mechanisms of disinhibition allow touch to instead directly activate pain circuits. Experimental evidence consistent with this theory has demonstrated the existence of a dorsally-directed polysynaptic pathway for mechanical pain that cannot be activated by innocuous mechanical input (touch) under normal conditions, due to a surrounding feed-forward inhibition, or "gate" (Duan et al., 2014; Lu et al., 2013; Torsney and MacDermott, 2006). Upon injury, various mechanisms trigger disinhibition, thus opening the gate and allowing the low threshold mechanoreceptors to engage the polysynaptic network to activate nociceptive-specific projection neurons in lamina I (Baba et al., 2003; Miraucourt et al., 2007; Torsney and MacDermott, 2006; Zeilhofer et al., 2012). This model provides a framework to begin to understand the anatomical substrates and mechanisms underlying mechanical allodynia, but we still do not know many of the fundamental aspects of the circuit, such as the identity of the neurons involved or how the circuit is organized.

Vesicular glutamate transporters (VGLUTs) package glutamate into synaptic vesicles for regulated release. We previously reported that VGLUT3, which has a relatively sparse distribution in the nervous system, is required specifically for acute mechanical pain and the persistent mechanical pain that develops in various models including inflammatory and neuropathic pain (Seal et al., 2009). All other somatosensory behaviors tested in mice lacking the transporter are normal, including thermal, itch, touch and persistent heat hypersensitivity.

Here, we took advantage of the specific requirement for VGLUT3 in mechanical pain to explore the cellular basis of the circuit using a number of complementary approaches. From the analyses, we have now identified a discrete population of spinal cord excitatory interneurons as the origin of the mechanical pain defects in VGLUT3 knockout (KO) mice. Interestingly, the cells reside in lamina III, a region important for touch, but largely ignored with respect to pain (but see Polgar et al., 2007a). We now also show that the cells participate in the persistent mechanical pain circuit and receive almost exclusively low threshold input, thus positioning them at a critical entry point to the circuit. We also identified additional excitatory populations that participate in the dorsal horn circuit for persistent mechanical hypersensitivity, including neurons in inner lamina II that express calretinin and were recently suggested to transmit only light acute mechanical pain (Duan et al., 2014). Lastly, we provide evidence that the neuronal composition of the circuit differs for different types of injury, indicating the existence of microcircuits for mechanical hypersensitivity. A better understanding of the microcircuits and their relationship to the injury will lead to more effective treatment strategies.

RESULTS

Characterization of Conditional VGLUT3 KO Mice

To identify the locus of the acute and persistent mechanical pain defects observed in global VGLUT3 KO mice, we used our floxed conditional KO line ($VGLUT3^{fl/fl}$) (Figure S1A). Western blot analysis on brain lysates and immunohistochemistry performed on spinal cord slices from homozygous floxed mice indicate that VGLUT3 levels are not altered by loxP insertion (Figures S1B and S1C). We also produced a germline deletion,

VGLUT3$^{\Delta/\Delta}$, by crossing VGLUT3$^{fl/fl}$ to CMV^{Cre} mice. Biochemical and immunohistochemical analyses confirmed that this mouse line does not express the transporter (Figures S1B and S1C). Importantly, the VGLUT3$^{\Delta/\Delta}$ mice show attenuated acute mechanical pain in the Randall-Selitto assay as well as significantly reduced mechanical hypersensitivity in both the carrageenan model of inflammatory pain and the spared nerve injury (SNI) model of neuropathic pain (Figure S1D), similar to VGLUT3 global KO mice (Seal et al., 2008; Seal et al., 2009).

Cellular Origin of the Mechanical Pain Defects in VGLUT3 KO Mice

In adult mouse spinal cord, VGLUT3 is largely restricted to a discrete population of dorsal root ganglion (DRG) neurons, the C-low threshold mechanoreceptors (C-LTMRs) that innervate dorsal horn lamina II (Figure S1C) (Seal et al., 2009). To assess whether mechanical pain sensation requires VGLUT3 expression by these cells, we deleted the transporter in all DRG neurons using Advillin^{Cre} mice (Figures 1A-1D). This line expresses Cre only in DRG and not spinal cord or brain (Figure 1A) (Hasegawa et al., 2007). Indeed, when the Advillin^{Cre} mouse was crossed to the lsl-tdTomato reporter (Madisen et al., 2010) all DRG neurons expressed tomato (Figure 1B). As expected, VGLUT3 immunoreactivity was not detected in the dorsal horn of adult VGLUT3$^{fl/fl}$;Advillin^{Cre} mice (Figure 1C). Tail withdrawal thresholds of VGLUT3$^{fl/fl}$;Advillin^{Cre} mice did not differ from those of VGLUT3$^{fl/fl}$ control mice (Figure 1D), indicating that loss of VGLUT3 from DRG does not affect acute mechanical pain sensation. In both the carrageenan and SNI models, the ipsilateral paw withdrawal thresholds of the VGLUT3$^{fl/fl}$;Advillin^{Cre} mice were similar to VGLUT3$^{fl/fl}$ control mice and

significantly reduced compared to the contralateral paw (Figure 1D), indicating that loss of VGLUT3 in DRG also does not affect mechanical hypersensitivity. Consistent with these results, loss of VGLUT3 from unmyelinated DRG neurons, including the C-LTMRs, using the SNS^{cre} line (Agarwal et al., 2004) also did not alter mechanical pain behavior (Figures S1E-S1H).

Several brain regions implicated in pain processing express VGLUT3. Alternatively, dorsal horn neurons at early postnatal ages as well as Merkel cells, the end organ of slowly adapting mechanoreceptors, also express the transporter (Lou et al., 2013). To address whether VGLUT3 expressed by either of the latter two populations has a role in mechanical pain, we generated $VGLUT3^{fl/fl}$;$Hoxb8^{Cre}$ mice (Figures 1E-1H). $Hoxb8^{Cre}$ mice express Cre in all neurons that lie caudal to cervical level 2-3, and not in the brain (Figure 1E) (Witschi et al., 2010). Immunoreactivity for VGLUT3 in the $VGLUT3^{fl/fl}$;$Hoxb8^{Cre}$ mouse was absent from the lumbar dorsal horn, but still present in the striatum (Figures 1F and 1G). Withdrawal thresholds in both the acute and persistent mechanical pain assays were all markedly elevated in these mice compared to $VGLUT3^{fl/fl}$ controls (Figure 1H). To delete VGLUT3 specifically in Merkel cells, we crossed the $VGLUT3^{fl/fl}$ mice to the $KRT14^{Cre}$ line (Figure 1I), a line that expresses Cre specifically in keratinocytes and Merkel cells (Figures 1J and 1K) (Hafner et al., 2004). Mechanical pain behavior in $VGLUT3^{fl/fl}$;$KRT14^{Cre}$ mice was similar to control $VGLUT3^{fl/fl}$ mice (Figure 1L). Taken together these data point to dorsal horn neurons as the likely locus of the pain defects.

Dorsal Horn Neurons Underlie the Defects in Mechanical Pain

To examine the distribution of neurons that transiently express VGLUT3 in the dorsal horn, we crossed our BAC transgenic VGLUT3^{Cre} mice (Grimes et al., 2011) to the lsl-tdTomato mice. The resulting mice show both the adult and developmental expression of VGLUT3, as tomato is present in all cells that have ever expressed Cre. In the dorsal horn, tomato^{+} neurons are present in lamina III and to a lesser extent lamina II (Figure 2A). We also examined the dorsal horn of the VGLUT3^{EGFP} BAC transgenic line, in which EGFP expression is under the direct control of VGLUT3 regulatory elements (Figure 2B) (Seal et al., 2009). In this line, we observe a peak number of EGFP^{+} cells at postnatal day (P) 10-12, but the reporter is present only in the central terminals of C-LTMRs in the adult (Figure 2B). We also analyzed VGLUT3 expression in the dorsal horn directly by taking advantage of the VGLUT3$^{fl/fl}$;Advillin^{Cre} mice. Because VGLUT3 is deleted from primary afferents in these mice, expression is thus restricted to spinal cord neurons. Here we observed VGLUT3 immunoreactivity that first appeared around P5, peaked around P10-12 and was significantly reduced by ~P20 (Figure 2C).

To determine whether mechanical pain sensation requires the transient expression of VGLUT3 by dorsal horn neurons, we used Lbx1^{Cre} mice. In this line, Cre is restricted to only spinal cord dorsal horn neurons and is not in DRG or brain (Figure 2D) (Sieber et al., 2007). To confirm that the VGLUT3^{+} cells are in the Lbx1^{Cre} lineage, we generated VGLUT3^{EGFP};lsl-tdTom;Lbx1^{Cre} mice. Virtually all EGFP^{+} cells in the dorsal horn expressed tomato at P10 (Figure 2E). Importantly, no DRG neurons expressed tomato (Figure 2F). Consistent with the deletion of VGLUT3 in the dorsal horn and not in DRG, VGLUT3 immunoreactivity in VGLUT3$^{fl/fl}$;Lbx1^{Cre} mice at P10 appeared only as a discrete band in lamina II$_i$ corresponding to C-LTMR afferents

(Figure 2G). In the acute mechanical pain assay, tail withdrawal thresholds were significantly elevated compared to VGLUT3$^{fl/fl}$ controls (Figure 2H). Additionally, in the carrageenan and the SNI models of persistent pain, the von Frey thresholds of VGLUT3$^{fl/fl;}$Lbx1^{Cre} mice were significantly higher than control mice after injury. As expected, heat hypersensitivity, which is unaffected in global VGLUT3 KO mice, did not differ from controls. These data confirm that the dorsal horn neurons are the locus of the acute and persistent mechanical pain defects observed in global VGLUT3 KO mice.

To determine in more detail the mechanosensory behaviors that require VGLUT3, we tested the mice in several additional assays. VGLUT3$^{fl/fl}$;Lbx1^{Cre} showed reduced pinprick pain and impaired dynamic mechanical allodynia after carrageenan injection, but showed normal light touch-related behavior in the sticky tape and hair clip assays (Figure 2H).

VGLUT3 Marks a Population of Excitatory Interneurons in the Dorsal Horn

To determine whether VGLUT3 is expressed by inhibitory or excitatory interneurons, we performed double fluorescent *in situ* hybridizations on lsl-tdTom;VGLUT3^{Cre} mice. Nearly all *tomato*$^{+}$ cells co-expressed the excitatory (*vglut2*) and not the inhibitory marker (*gad67*) (Figure 3A). Tomato^{+} cells also did not express Pax2, another marker of inhibitory neurons (Figure 3B). To confirm that the mechanical pain defects are due to the loss of VGLUT3 from the excitatory neurons, we generated VGLUT3$^{fl/fl}$;Tlx3^{Cre} mice (Figures 3C-3E), in which Cre is only expressed by excitatory neurons (Xu et al., 2013). Immunoreactivity for VGLUT3 was absent in the dorsal horn of these mice at P10 (Figure 3D). In all three mechanical pain assays, withdrawal thresholds were

significantly elevated compared to VGLUT3$^{fl/fl}$ controls (Figure 3E), consistent with the behavior of global VGLUT3 KO and VGLUT3$^{fl/fl}$;Lbx1^{Cre} mice.

To further identify the transient VGLUT3 neurons, we examined co-expression of tomato with dorsal horn markers in lsl-tdTom;VGLUT3^{Cre} mice (Figures 3F and 3G). At peak VGLUT3 expression (P10), few tomato^{+} cells express PKCγ (16%; 212 of 1311) or calretinin (10%; 108 of 1209). Similarly, tomato overlaps with ~25% (212 of 815) of the PKCγ population, and only 7% (108 of 1469) of calretinin neurons. The degree of overlap is similar in the adult.

Architecture and Afferent Innervation of the VGLUT3 KO Spinal Cord

Gross anatomical defects, such as the aberrant innervation by central terminals of DRG neurons or the loss of spinal cord neurons have been observed in mouse mutants with spinal cord gene deletions (Ross et al., 2010; Wang et al., 2013; Xu et al., 2013). Such changes could potentially contribute to disruption of the mechanical pain circuit in VGLUT3 KO mice. We therefore examined the distribution of molecular markers for spinal cord neurons (NeuN, vesicular GABA transporter, NK1R, VGLUT2 and PKCγ) and primary afferents (TRPV1, CGRP, isolectin-B4 and VGLUT1) in the dorsal horn of VGLUT3 KO and WT mice (Figure S2A) but observed no major differences. Crossed onto the global VGLUT3 KO strain, lsl-tdTom;VGLUT3^{Cre} mice showed no change in the number of tomato^{+} dorsal horn neurons compared to mice WT for VGLUT3 (Figures S2B-S2C). Thus, deletion of VGLUT3 does not cause apoptosis or obvious changes in the architecture or afferent innervation of the dorsal horn, consistent with a more discrete defect in synaptic transmission.

Synaptic Transmission Defect is Consistent with Attenuated Mechanical Allodynia

The anatomical basis for light touch becoming painful after injury is thought to involve a disinhibition of the dorsal horn mechanical pain circuits that allows low threshold mechanoreceptors to activate pain transmitting projection neurons in lamina I ($NK1R^+$) through a dorsally-directed polysynaptic network (Braz et al., 2014). Since the loss of VGLUT3 from dorsal horn excitatory neurons causes a behavioral impairment in mechanical hypersensitivity, we hypothesized that the low threshold A-fibers would not activate nociceptive lamina I neurons under conditions of disinhibition (the injured state) in the KO mice. To test this hypothesis, we used an *in vitro* spinal cord model of mechanical allodynia (Torsney and MacDermott, 2006). In this model, when inhibitory tone is normal, dorsal root stimulation at A-fiber intensities is unable to generate polysynaptic excitatory currents in nociceptive lamina I projection neurons. However, under pharmacological disinhibition, stimulation of the dorsal roots at A-fiber intensity reliably generates polysynaptic excitatory currents in the lamina I projection neurons, thus serving as the anatomical substrate for the perception of touch as painful after injury (Baba et al., 2003; Miraucourt et al., 2007; Torsney and MacDermott, 2006). This model is illustrated in Figure 4A.

Whole-cell patch clamp recordings were performed in transverse spinal cord slices with dorsal roots and DRGs still attached (Figure 4B). Roots were electrically stimulated at different intensities to recruit Aβ (25 μA) or Aβ and Aδ (100 μA) or Aβ, Aδ and C fibers (500 μA), respectively. To visualize neurons expressing NK1R, slices were

pre-incubated with the fluorescent tetramethylrhodamine substance P conjugate, SP-TMR (Figure 4C) as previously described (Torsney and MacDermott, 2006). Under normal conditions, Aδ- and C-, but not Aβ-fiber stimulation produced monosynaptic glutamatergic EPSCs in $NK1R^+$ lamina I neurons of both global VGLUT3 KO and control mice, similar to what has been observed in rats (Figure 4D, left traces) (Torsney and MacDermott, 2006). In the presence of the inhibitory receptor antagonists bicuculline (10 μM) and strychnine (300 nM), stimulation of dorsal roots at Aβ intensity reliably produced polysynaptic EPSCs in $NK1R^+$ lamina I neurons in slices from WT mice (Figure 4D, upper right traces and Figure 4E). We also occasionally observed Aδ-induced polysynaptic EPSCs consistent with previous observations (Figure S2D) (Torsney and MacDermott, 2006). Strikingly, stimulation at A-fiber intensities failed to produce polysynaptic EPSCs in lamina I neurons of VGLUT3 KOs (Figure 4D, bottom right traces and Figure 4E). As a control, increasing the intensity of stimulation to recruit all A-fibers (100 μA) or all types of fibers (500 μA) produced monosynaptic EPSCs in the $NK1R^+$ neurons similar to those observed in the absence of inhibitory blockers, showing that deletion of VGLUT3 selectively eliminated the polysynaptic EPSCs induced by Aβ-fibers. Importantly, conduction velocities as well as afferent thresholds measured for Aδ- and C-fibers did not differ between VGLUT3 KO and WT mice (Aδ threshold, 100 μA, $p = 0.34$; C threshold, 500 μA, $p = 0.46$; Figure S2E) and were similar to values previously reported (Torsney and MacDermott, 2006). The results are consistent with a severe impairment in neuronal transmission within the dorsal horn polysynaptic pathway that conveys mechanical hypersensitivity. In addition, the data

provide support for altered excitatory transmission rather than a compensatory up-regulation of inhibition.

VGLUT3^{+} Dorsal Horn Neurons Convey Mechanical Hypersensitivity

Our results show that normal mechanical pain sensation requires the transient postnatal expression of VGLUT3 by dorsal horn neurons, raising the possibility that the neurons themselves convey this type of pain. To test this hypothesis, we used a chemogenetic approach, targeting the excitatory designer receptor (DREADDs) hM3Dq to Cre expressing cells in lamina III of the VGLUT3^{Cre} mice and then assessing whether activation of the cells with the receptor-specific ligand, clozapine-n-oxide (CNO), produces mechanical allodynia. First we verified that the Cre^{+} cells in the dorsal horn of our transgenic line match those responsible for the mechanical pain defects in VGLUT3 KO mice (Figures S3A and S3B). In the Randall-Selitto, carrageenan and SNI mechanical pain assays, VGLUT3$^{fl/fl}$;VGLUT3^{Cre} mice showed significantly elevated withdrawal thresholds compared to control mice (Figure S3B). Because all adult dorsal horn excitatory neurons express VGLUT2, we predicted that deletion of VGLUT2 from the transient VGLUT3 cells would also produce the mechanical pain defects (Figure S3C). Interestingly, while persistent mechanical hypersensitivity was reduced in the VGLUT2$^{fl/fl}$;VGLUT3^{Cre} mice (similar to knocking out VGLUT3), acute mechanical pain was normal. This unexpected finding is consistent with the idea that although both acute and persistent mechanical pain require the transient postnatal expression of VGLUT3 by these dorsal horn neurons, the cells themselves only transmit persistent pain in the adult.

To target the hM3Dq receptor specifically to the dorsal horn, we used a viral approach. We first determined that the AAV8 serotype coupled with the neuron-specific human synapsin promoter was highly specific for the infection of only dorsal horn neurons (and not DRG) (Figure S4). Three weeks after injection of the AAV8-hSyn-DIO-hM3Dq-mCherry virus into one side of the lumbar enlargement of P10 VGLUT3^{Cre} mice (when Cre is at peak expression), the reporter was highly restricted to neurons in lamina III and importantly was not present in PKCγ neurons or DRG (Figures 5A and 5B). To confirm that hM3Dq functions properly in the dorsal horn, we performed patch clamp recordings in transverse spinal cord slices. As expected, application of 3 mM CNO produced an inward current in voltage clamp and generated action potentials in current clamp only in mCherry^{+} neurons (Figures 5C and 5D).

To test whether chemogenetic activation of the cells elicits mechanical pain behavior, we measured von Frey thresholds in the presence and absence of CNO (Figure 5E). In the absence of CNO, thresholds for both hindpaws were similar, suggesting that viral infection alone does not affect mechanical sensitivity. After CNO injection, thresholds were dramatically reduced at only the ipsilateral hindpaw, consistent with the induction of mechanical hypersensitivity. The injected mice also showed guarding and occasional fluttering of the ipsilateral hindpaw upon contact with an innocuous surface, indicative of mechanical allodynia (Figure 5F; Movie S1). In a test of heat hypersensitivity (Figure 5E), which is not altered in the global VGLUT3 KO, withdrawal latencies were the same for both hindpaws before and after CNO injection. Since deletion of VGLUT3 in these neurons impairs mechanical hypersensitivity (Figure S3B), we hypothesized that mice lacking the transporter would not show the drop in

threshold. Indeed, injection of CNO in VGLUT3$^{fl/fl}$;VGLUT3^{Cre} mice expressing hM3Dq did not alter the mechanical threshold (Figure 5E). The mice also showed essentially no paw fluttering and significantly less guarding behavior compared to VGLUT3^{Cre} mice (Figure 5F; Movie S1). The data thus provide strong evidence that transient VGLUT3 neurons in lamina III participate in the circuit for mechanical hypersensitivity.

c-Fos Reveals the Dorsally-directed Pathway For Mechanical Hypersensitivity

To identify additional dorsal horn neurons that participate in the mechanical allodynia circuit, we stained for c-Fos, a marker of neuronal activity, after activation of hM3Dq in VGLUT3^{Cre} mice. After injection of CNO in anesthetized mice, c-Fos was surprisingly restricted almost exclusively to the mCherry^{+} cells (Figure 5G; Figure S5). This was also observed with the VGLUT3$^{fl/fl}$;VGLUT3^{Cre} mice. Since mechanical hypersensitivity in the VGLUT3^{Cre} mice requires low threshold input, we followed CNO injection with walking the mice at a pace that was slow, but avoided guarding behavior. Under these conditions, a dramatic increase in c-Fos^{+} cells was observed in laminae I-II and to a lesser degree in lamina III in VGLUT3^{Cre}, but not VGLUT3$^{fl/fl}$;VGLUT3^{Cre} mice (Figures 5G and 5H; Figure S5). Importantly, c-Fos expression was increased predominantly in the medial dorsal horn, an area corresponding to the distal part of the limb. Mice that did not receive CNO showed little to no c-Fos in the dorsal horn and mice that received mechanical stimulation, but not CNO, showed c-Fos only in deeper laminae, where innocuous mechanical circuits are active (Figure 5G; Figure S5).

To further identify the c-Fos^{+} neurons in laminae I-III, we co-stained for PKCγ, calretinin and Pax2. The c-Fos co-stained with ~48% of mCherry^{+}, 21% of PKCγ^{+}, 28%

of calretinin^{+} and 14% of Pax2^{+} neurons (Figure 5I). Interestingly, c-Fos was also induced in an excitatory population in lamina III that lacked mCherry and PKCγ. Thus, we have now identified at least four distinct excitatory interneuron populations that reside within the circuit for mechanical hypersensitivity.

To identify neurons postsynaptic to the transient VGLUT3 population in lamina III, we injected a Cre-dependent virus encoding the anterograde trans-neuronal tracer, wheat-germ agglutinin (WGA) (Braz et al., 2002) in lsl-tdTom;VGLUT3^{Cre} mice at P10 (Figure S6). WGA allowed us to refine the position of the neurons with respect to the VGLUT3^{Cre} cells by observing the location of the tracer across time. At the earliest time point (3 dpi), WGA was detected almost exclusively in lamina III tomato^{+} neurons and not DRG. On days 4 and 5, we detected additional neurons in laminae III and IV as well as vertical cells in lamina II_o, which are all likely to be directly postsynaptic. By 6 and 21 dpi, WGA was still excluded from DRG, but was now detected in lamina II where it co-localized with PKCγ and calretinin as well as with inhibitory neurons throughout laminae II-III. We thus conclude that within lamina III, the transient VGLUT3 population is presynaptic to another unidentified population of excitatory neurons, which are presynaptic to lamina II calretinin and PKCγ neurons.

VGLUT3^{+} Lamina III Cells Receive A-fiber Input

We next determined whether the transient VGLUT3 cells in lamina III directly receive low threshold input, a key component of the dorsal horn circuit for mechanical allodynia (Braz et al., 2014). Using lsl-tdTom;VGLUT3^{Cre} mice, we recorded lamina III tomato^{+} neurons which exhibited equally phasic or tonic firing patterns in response to current

injection (Figures 6A and 6B). Remarkably, dorsal root stimulation at A-fiber intensity induced EPSCs in all recorded tomato^{+} neurons (Figures 6C and 6D). About half of the cells (46%) received combined direct monosynaptic Aβ and polysynaptic Aδ inputs and a few received polysynaptic C-fiber input. The high proportion of cells receiving direct A-fiber input together with the behavioral results, suggest that the transient VGLUT3 population serves as an entry point to the A-fiber mediated, dorsally-directed circuit for mechanical allodynia.

Subsequent morphological analyses revealed that the neurons are fairly homogeneous, showing a predominantly dorso-ventral dendritic arbor. Very few cells have a radial morphology and none resemble central or islet cells (Figure 6E). This finding is consistent with previous reports describing Lamina III excitatory interneurons with dorsally-directed processes (Polgar et al., 2007b; Schneider, 2008). Both phasic and tonic neurons showed similar morphologies and afferent input, but phasic neurons were more uniform with only dorsally-directed dendrites.

Lamina II Calretinin^{+} Neurons Convey Mechanical Hypersensitivity

Mechanical allodynia resulting from activation of the transient VGLUT3 neurons induced c-Fos expression in calretinin neurons, suggesting that these cells also transmit mechanical hypersensitivity. A small proportion of calretinin cells also transiently express VGLUT3 (Figure 3). We therefore first tested acute and persistent pain behaviors in VGLUT3$^{fl/fl}$;CR^{Cre} mice, but observed no difference compared to VGLUT3$^{fl/fl}$ controls (Figures S7A and S7B).

To directly manipulate calretinin neurons, we injected the hM3Dq virus into the dorsal horn of CR^{Cre} mice (Figure 7A). Expression of the mCherry was limited to a discrete layer of calretinin$^+$ cells within the dorsal part of lamina II_i and was absent from PKCγ and DRG neurons (Figure 7B; Figures S7C and S7D). Importantly, mCherry expression corresponded to calretinin$^+$ cells in the adult and not to neurons in lamina I, II_o and the ventral part of lamina II that transiently express calretinin during development and can be observed in lsl-tdTom;CR^{Cre} mice (Figure S7E). These adult calretinin neurons are largely distinct from an Lbx1$^+$ population (Figure S7F) recently shown to affect acute pain (Duan et al., 2014). After CNO injection, the ipsilateral von Frey threshold dropped dramatically (Figure 7D). Behaviors such as paw guarding and fluttering were also observed in the ipsilateral paw (Figure 7E; Movie S2) consistent with mechanical hypersensitivity and similar to what we observed with $VGLUT3^{Cre}$ mice. Thermal sensitivity in these mice was unchanged (Figure 7D).

We also examined the dorsal horn expression of c-Fos in these mice. In anesthetized animals injected with CNO, c-Fos was induced primarily in mCherry$^+$ cells (Figures 7F and 7G; Figure S7G). However, coupling low threshold mechanical stimulation with CNO dramatically increased the number of c-Fos neurons in laminae I-II (Figures 7F and 7G; Figure S7H). This increase was absent in mice lacking hM3Dq or injected with saline (Figure 7G).

To further characterize the c-Fos$^+$ cells, we co-stained for calretinin, PKCγ and Pax2 (Figure 7H). Approximately 30% of the calretinin neurons expressed mCherry and half of these showed c-Fos induction. Of the remaining mCherry-negative calretinin neurons, ~45% expressed c-Fos indicating a high degree of activation within the

calretinin population. We also observed ~30% of c-Fos$^+$ cells co-stained with Pax2. Most interestingly, very few of the c-Fos$^+$ cells co-stained for PKCγ.

Our data thus far show that hM3Dq activation of either the transient VGLUT3 neurons in lamina III or the adult calretinin neurons in lamina II produces mechanical hypersensitivity, and that coupling a mechanical stimulus to the activation of these cells induces c-Fos in the dorsal horn circuit for mechanical allodynia. Interestingly, activation of the transient VGLUT3, but not the calretinin neurons, produces c-Fos in PKCγ neurons, suggesting the existence of more than one allodynic pathway. Since the discovery of PKCγ as a critical component of persistent mechanical pain (Malmberg et al., 1997), evidence for its contribution to allodynia produced by different types of injury has remained unclear (Gao and Ji, 2010; Zhao et al., 2011; Zou et al., 2011). We therefore compared the pattern of c-Fos induction in the carrageenan and SNI models (Figures 8A-8F).

Lsl-tdTom;VGLUT3^{Cre} mice were injected with carrageenan with or without low threshold mechanical stimulation 24 hours later. As expected, the number of c-Fos$^+$ cells in laminae I-III was increased dramatically in the mice that also received mechanical stimulation (Figures 8A and 8B). The distribution of c-Fos was strikingly similar to what was observed by activating the calretinin population together with mechanical stimulation, including a number of calretinin (~17%) and Pax2 (~41%) cells, but very few PKCγ neurons (~1%) (Figure 7H). Additionally, a significant number of c-Fos$^+$ cells co-expressed tomato (16%), indicating activation of the transient VGLUT3 population.

For the SNI model, mice that received mechanical stimulation three days after surgery showed a substantial increase in c-Fos$^+$ cells in laminae I-II (Figures 8D and 8E). In contrast to the inflammatory pain model, a significant number of PKCγ (11%) and fewer calretinin (8%) neurons expressed c-Fos (Figure 8F). Again, a substantial number of c-Fos$^+$ cells co-expressed tomato (~11%). Together, our data show that distinct spinal circuits can lead to mechanical allodynia, with both requiring activation of the transient VGLUT3 neurons.

DISCUSSION

This study shows that the critical role of VGLUT3 in mechanical pain arises from its transient expression by dorsal horn excitatory interneurons. The cells directly receive Aβ primary sensory input and are required for polysynaptic transmission onto lamina I pain processing neurons after injury. Chemogenetic activation of transient VGLUT3 neurons in lamina III induces mechanical allodynia in a circuit that also includes PKCγ and calretinin cells in lamina II. Activation of calretinin neurons also induces mechanical hypersensitivity and engages a distinct, dorsally-directed pathway that does not include the PKCγ neurons. Further, we show that mechanical allodynia observed in models of inflammation and neuropathy is mediated by distinct neural circuits. Both require the participation of transient VGLUT3 neurons, but a distinct complement of second order neurons.

Role of VGLUT3 in the somatosensory system

Although VGLUT3 expression in the dorsal horn of adult mice is restricted to C-LTMRs, we now show that loss of the transporter from this population does not produce the mechanical pain defects observed in global VGLUT3 KO mice. Using a conditional VGLUT3 KO and several Cre-driver lines, including the spinal cord specific driver $Lbx1^{Cre}$, we have determined that the defects are due to the loss of VGLUT3 from spinal cord neurons that express the transporter transiently during postnatal development. The finding, however, does not address whether the C-LTMRs themselves are important for pain. These DRG neurons also express VGLUT2 and tyrosine hydroxylase, which may provide alternative mechanisms for signaling (Li et al., 2011; Scherrer et al., 2010). Studies in humans and rodents suggest C-tactile afferents transmit pleasant touch sensation under normal conditions (Loken et al., 2009; Vrontou et al., 2013) and may have a role in suppressing pain potentially by activating islet cells (but also see Nagi *et al*) (Delfini et al., 2013; Liljencrantz et al., 2013; Nagi et al., 2011). Consistent with this idea, the C-LTMRs do not contact the pain-promoting PKCγ neurons that also reside in this layer (Peirs et al., 2014).

Our analysis of the dorsal horn architecture, including the pattern of primary afferent innervation and electrophysiological properties, showed no evidence of gross abnormalities in the VGLUT3 KO mice. However, using an *in vitro* model of mechanical allodynia, we find that low threshold A-fibers are unable to activate $NK1R^{+}$ lamina I neurons when inhibitory transmission in the dorsal horn is completely blocked, indicating that the loss of mechanical hypersensitivity reflects a profound impairment in excitatory transmission between second order neurons. Interestingly, a small decrease in excitatory transmission in this polysynaptic pathway, such as blocking only NMDA

receptors, can also prevent the activation of lamina I neurons (Torsney and MacDermott, 2006). Thus, a local change in synaptic transmission due to the absence of VGLUT3 could have a dramatic downstream impact. Importantly, the transient expression of VGLUT3 coincides with a critical period in the maturation of the dorsal horn, a time when the interneurons are establishing their mature firing patterns and connectivity (Fitzgerald, 2005). At the synaptic level, both NMDA and AMPA receptors are undergoing a series of changes, including the awakening of silent synapses and activity dependent alterations in subunit composition (Baba et al., 2000; Li and Zhuo, 1998). Precisely how VGLUT3 participates in these or other developmental changes to properly setup the mechanical pain circuit remains unclear and the subject of further investigation.

Spinal cord circuit for mechanical hypersensitivity

Original models of the dorsal horn circuit for mechanical allodynia have focused almost exclusively on a series of synaptically connected neurons that transmit touch information to superficial layers (Lu et al., 2013; Miraucourt et al., 2007; Torsney and MacDermott, 2006). This serial circuit starts with PKCγ neurons, which then activate central cells in lamina II_i, vertical cells in lamina II_o, and finally the lamina I projection neurons (Lu et al., 2013; Lu and Perl, 2005). More recently, additional circuits have been proposed (Braz et al., 2014; Yasaka et al., 2014) to support the idea that the induction and transmission of mechanical hypersensitivity within the dorsal horn involves integrating information through multiple mechanisms and neuronal networks.

Surprisingly, deep dorsal horn neurons, which receive the major input from low-threshold sensory neurons, have been largely ignored. We now show using a chemogenetic approach that the transient VGLUT3 neurons located in lamina III directly participate in the mechanical allodynia circuit. Interestingly, although loss of VGLUT3 from the laminae II-III dorsal horn neurons attenuates both acute and persistent pain, deletion of VGLUT2, the transporter that mediates glutamate signaling by these neurons in the adult, produces defects only in persistent mechanical pain, suggesting that the neurons themselves do not convey acute mechanical pain. This result is consistent with the lack of acute pain behavior (biting and licking) observed when we activate hM3Dq in the VGLUT3^{Cre} mice. The paw guarding and fluttering behavior that we do observe in these mice is more consistent with the actions of a limb sensitive to touch.

We also now report that activation of calretinin neurons in lamina II of adult mice specifically induces mechanical allodynia. These neurons are distinct from the calretinin population recently shown to be important only for light mechanical pain (Duan et al., 2014). Thus, there are at least two distinct calretinin populations in lamina II, one that transiently expresses calretinin together with Lbx1 and is not involved in mechanical hypersensitivity, and a second population that permanently expresses calretinin, but never Lbx1 and is important for persistent mechanical pain. Additionally, the adult calretinin population as well as the transient VGLUT3 population are distinct from the somatostatin^{+} excitatory neurons in lamina II that express Lbx1, partially overlap with PKCγ neurons and likely vertical cells (Duan et al., 2014; Polgar et al., 1999) and were recently implicated in persistent mechanical pain.

The transient VGLUT3 cells in lamina III receive input from myelinated Aβ fibers,

placing them at an entry point for the dorsally-directed mechanical allodynia circuit. The anterograde tracing and c-Fos results provide a map of the rest of the allodynia circuit starting from these lamina III transient VGLUT3 neurons. Interestingly, we find that the neurons are connected to a second population of excitatory interneurons in this same lamina. These latter, still unidentified neurons, likely serve as the connection between lamina III and the more dorsally located neurons in the pathway including PKCγ and calretinin neurons. The tracing study also shows a direct connection between the transient VGLUT3 neurons and cells in lamina II_o, which are likely to be vertical cells because unlike other neurons in lamina II, these cells have long ventrally-directed dendrites that reach into lamina III. Consistent with our observation, Kato et al identified a population of lamina III excitatory neurons that provides a major input to the lamina II vertical cells and thus a potentially shorter route to the nociceptive projection neurons (Kato et al., 2009).

It has been suggested that the dorsal horn circuit for mechanical allodynia is controlled by a feed-forward inhibition evoked by low threshold inputs that prevent touch from becoming painful (Braz et al., 2014; Zeilhofer et al., 2012). This concept has elicited much interest, as it is the central element of “the gate control theory of pain” published by Melzack and Wall in 1965. In this model, revisited in recent reviews (Braz et al., 2014; Zeilhofer et al., 2012), the “gate” represents a population of inhibitory interneurons that facilitate nociceptive circuits and also prevent the passage of touch-related information from deep neurons to more superficial pain-processing cells. PKCγ-expressing neurons reside at the border between touch and pain (lamina II_i) and have been suggested to be key elements of the circuit (Lu et al., 2013; Miraucourt et al.,

2007). The cells have been modeled as initiating the activation of a dorsally-directed pathway transforming touch into pain when the “gate is opened”, i.e. when the inhibition controlling their activity is decreased by injury. Our data now refines how these neurons participate in mechanical allodynia. Firstly, we now show that neurons more ventrally-located than the PKCγ neurons are required to elicit mechanical pain behavior in the carrageenan and SNI models as well as to evoke EPSCs in lamina I in the *in vitro* assay of mechanical allodynia. Interestingly, these transient VGLUT3 neurons do not show evidence of being under significant feed-forward inhibition as they reliably exhibit evoked EPSCs and membrane depolarization upon dorsal root stimulation. Thus, although these neurons are likely to engage the pathway, the nexus of inhibition must instead be on the postsynaptic lamina III neurons or the excitatory populations in lamina II (Duan et al., 2014) including the PKCγ neurons, which are known to be under strong inhibitory control (Lu et al., 2013). Secondly, we observed c-Fos expression in PKCγ neurons in the SNI model of neuropathic pain, but not the carrageenan model of inflammatory pain suggesting that the involvement of these neurons in the two models of mechanical hypersensitivity may differ. The precise role of PKCγ neurons in different types of injury will require further investigation. From this work, we now propose that the mechanical allodynia circuit is composed of multiple overlapping microcircuits with distinct gates that are engaged by different types of injuries (See model in Figure 8). The more comprehensive view of the spinal cord circuitry provided by this study will help guide efforts to design and implement new treatment strategies.

EXPERIMENTAL PROCEDURES

Animals

Mice were treated in accordance with protocols approved by the Institutional Animal Care and Use Committee at the University of Pittsburgh. Conditional VGLUT3 KO mice ($VGLUT3^{fl/fl}$) were crossed to the $Rosa26^{Cre}$ line to generate $VGLUT3^{\Delta/\Delta}$ and to $Advillin^{Cre}$, $Hoxb8^{Cre}$, $KRT14^{Cre}$, $Tlx3^{Cre}$, $Lbx1^{Cre}$, SNS^{Cre} or $VGLUT3^{Cre}$ to generate cell-specific deletions. Detailed description of $VGLUT3^{fl/fl}$ and other mouse lines can be found in **Supplemental Experimental Procedures**.

Surgical procedures

SNI was preformed as previously described. Spinal cord injections of AAV were performed at P9-10 or P15-16. Under isoflurane, midline incision was made without laminectomy and virus delivered (1 µl) slowly with a glass microelectrode (50 µm tip) between lumbar segments L4-L5. Silk sutures were used to close *lassimus dorsi* and skin and Ketofen was given before and one day after surgery. Behavior was tested 3 weeks later. For more details including virus titers see **Supplemental Experimental Procedures**.

Electrophysiological Recordings and Morphology

Transverse slices were made from lumbar spinal cord of P25-35 mice, keeping roots and DRG attached. Whole cell patch-clamp recordings were made with neurobiotin in the pipette when morphology was also performed. For details see **Supplemental Experimental Procedures.**

In Situ hybridization and Immunohistochemistry

ISH and IHC were performed as previously described (Seal et al., 2009). Induction of c-Fos was performed under urethane anesthetic or with mechanical stimulation by slowly walking mice on a treadmill (10 cm/s). Mice were perfused with 4% paraformaldehyde 90 minutes after the treatment (see **Supplemental Experimental Procedures**).

Statistics

Data are reported as mean ± SEM. Randall-Selitto, pinprick, sticky tape and fur clip were analyzed by two-tailed Student's t-test. Von Frey, Hargreaves' and spontaneous behavior were analyzed by two-way ANOVA with Bonferroni's post-hoc test. Significance was considered $p < 0.05$.

SUPPLEMENTAL INFORMATION

Supplemental information includes 7 Figures and 2 Movies with Legends, Experimental Procedures and References.

AUTHOR CONTRIBUTIONS

CP, SPGW, XZ and RPS designed experiments, CP, SPGW, XZ, CW, JG, NC, ACG, ZL and PM performed experiments, HH provided a reagent, CP, SGW, XZ and RPS analyzed data and CP, SGW and RPS wrote the paper.

ACKNOWLEDGMENTS

We thank Dr. R. Kuner for SNS^{Cre} mice, Dr. F. Wang for $Advillin^{Cre}$ mice, Dr. H. Zeilhofer for $Hoxb8^{Cre}$ mice, Dr. Q. Ma for $Tlx3^{Cre}$ mice, Dr. C. Birchmeier for the $Lbx1^{Cre}$ mice, Dr. T. Hnasko for $VGLUT2^{fl/fl}$ mice and Dr. R. Sharif-Naeini for the WGA virus. We thank S. Dettwyler, J. Caverhill and C. Eckard for technical support, B. Sharif and Dr. Sharif-

Naeini for instruction on spinal cord injections, Dr. A. MacDermott for critical reading of the manuscript and the Pittsburgh Rodent Behavior Analysis Core. The work was funded by University of Pittsburgh Startup Funds, and grants from NINDs (NS084191), the UPMC Competitive Medical Research Fund, Virginia Kaufman Foundation, American Diabetes Foundation, Rita Allen Foundation and American Pain Society to RPS and China Scholarship Council Fellowship to XZ.

FIGURE LEGENDS

Figure 1. Mechanical Pain Defects Do Not Arise from DRG or Brain.

(A) Cartoon of Avil^{Cre} mice showing Cre (red) is restricted to primary afferents.

(B) All DRG neurons express tomato in lsl-tdTom;Avil^{Cre} mice.

(C) VGLUT3-IR is not detected in primary afferents (arrows) of VGLUT3$^{fl/fl}$;Avil^{Cre} in the adult.

(D) Paw withdrawal thresholds (PWT) of VGLUT3$^{fl/fl}$;Avil^{Cre} mice do not differ from control mice after carrageenan (n=12 both groups) or SNI (n=7 and n=9 respectively). Randall-Selitto thresholds also do not differ from controls (n=8 and n=6 respectively).

(E) Cartoon of Hoxb8^{Cre} mice showing Cre (red) is expressed by spinal cord and DRG neurons, but not brain.

(F) VGLUT3$^{fl/fl}$;Hoxb8^{Cre} mice lack VGLUT3-IR in the dorsal horn at p10.

(G) VGLUT3-IR is still present in the striatum of VGLUT3$^{fl/fl}$;Hoxb8^{Cre} mice.

(H) PWTs of VGLUT3$^{fl/fl}$;Hoxb8^{Cre} mice are significantly greater than controls after carrageenan (n=11 and n=9 respectively) and SNI (n=9 and n=4 respectively). Randall-Selitto thresholds are also significantly elevated compared to controls (n=9 and n=7).

(I) Cartoon of KRT14^{Cre} mice showing Cre (red) is restricted to keratinocytes and Merkel cells.

(J) As expected, tomato and the Merkel cell marker TROMA1-IR co-localize (arrowhead) in hindpaw glabrous skin of lsl-tdTom;KRT14^{Cre} mice.

(K) Tomato and TROMA1-IR also co-localize (arrowheads) in hindpaw glabrous skin of lsl-tdTom;VGLUT3^{Cre} mice.

(L) PWTs do not differ between VGLUT3$^{fl/fl}$;KRT14^{Cre} and control mice before or after carrageenan (n=10 and n=6 respectively) or SNI (n=3 both groups). Randall-Selitto thresholds also do not differ (n=7 and n=6 respectively).

All scale bars = 100 μm except in G (50 μm). Data are mean ± SEM. *$p < 0.05$, **$p \leq 0.01$, ***$p \leq 0.001$.

Figure 2. Somatosensory Behaviors of VGLUT3$^{fl/fl}$;Lbx1^{Cre} Mice.

(A) In lsl-tdTom;VGLUT3^{Cre} mice, tomato^{+} neurons are located in laminae II$_i$-III and 16% co-localize with PKCγ-IR (arrow).

(B) In VGLUT3^{EGFP} mice, EGFP is expressed by laminae II$_i$-III neurons at p10, but not adult.

(C) VGLUT3-IR in VGLUT3$^{fl/fl}$;Avil^{Cre} mice peaks around P10 (middle row).

(D) In Lbx1^{Cre} mice, only spinal cord neurons express Cre.

(E) EGFP and tomato co-localize at p10 in VGLUT3^{EGFP};lsl-tdTom;Lbx1^{Cre} mice (arrow). A few EGFP^{+} neurons at the lamina IV border do not express tomato^{+} (arrowhead).

(F) Tomato is not present in DRG of adult VGLUT3^{EGFP};lsl-tdTom;Lbx1^{Cre} mice.

(G) VGLUT3-IR in VGLUT3$^{fl/fl}$;Lbx1^{Cre} mice at P10 is present in primary afferents (arrow) and not spinal cord neurons.

(H) Baseline PWT of VGLUT3$^{fl/fl}$;Lbx1^{Cre} mice was similar to controls. After SNI (n=8 both groups), PWTs were significantly elevated compared to controls. Withdrawal responses in the Randall-Selitto assay (n=9 both groups) were also significantly higher than controls. After carrageenan, PWTs of VGLUT3$^{fl/fl}$;Lbx1^{Cre} mice (static mechanical) were elevated compared to controls (n=9 both groups). The mice also responded less frequently than controls to light dynamic mechanical stimulation with a cotton swab (n=11 and n=8 respectively). Latency to respond in the Hargreaves' test did not differ from controls (n=11 and n=8 respectively). VGLUT3$^{fl/fl}$;Lbx1^{Cre} mice responded less frequently than controls to pinprick of the plantar hindpaw (n=11 and n=8 respectively). Sticky tape and fur clip measures of touch did not differ between VGLUT3$^{fl/fl}$;Lbx1^{Cre} mice and controls (both tests n=8 and n=7 respectively).

All scale bars = 100 μm except inset in E (20 μm). Data are mean ± SEM. *$p<0.05$, **$p \leq 0.01$, ***$p \leq 0.001$.

Figure 3. Excitatory Neurons in the Dorsal Horn Transiently Express VGLUT3.

(A) *In situ* hybridization of *tomato* co-localized with *vglut2*, but not *gad67* in lsl-tdTom;VGLUT3^{Cre} mice.

(B) The inhibitory neuron marker Pax2 does not colocalize with tomato in lsl-tdTom;VGLUT3^{Cre} mice.

(C) Cartoon showing Tlx3^{Cre} mice express Cre (red) only in excitatory neurons in the dorsal horn, DRG neurons and sparsely in brain.

(D) VGLUT3$^{fl/fl}$;Tlx3^{Cre} mice at P10 lack VGLUT3-IR in the dorsal horn.

(E) Baseline PWTs of VGLUT3$^{fl/fl}$;Tlx3^{Cre} mice were similar to controls. After carrageenan (n=12 both groups) or SNI (n=11 and n=8 respectively), PWTs of VGLUT3$^{fl/fl}$;Tlx3^{Cre} mice were significantly elevated compared to controls, as were Randall-Selitto tail withdrawal thresholds (n=9 both groups).

(F) Co-localization of tomato and PKCγ in lsl-tdTom;VGLUT3^{Cre} mice at P10 and adult.

(G) Co-localization of tomato and calretinin in lsl-tdTom;VGLUT3^{Cre} mice at p10 and adult.

All scale bars = 100 μm except A and insets in B, F and G (20 μm). Data are mean ± SEM. **$p \leq 0.01$.

Figure 4. Loss of Polysynaptic Low Threshold Input to NK1R^{+} Lamina I Neurons.

(A) Schematic representation of the dorsal horn showing nociceptive inputs (High threshold (HT) C and Aδ fibers) to NK1R^{+} lamina I projection neurons (PN). Polysynaptic innocuous afferent (Low threshold (LT) Aβ and Aδ fibers) input to PNs through excitatory interneurons (Exc IN) is suppressed by local inhibitory interneurons (Inh IN). Disinhibition induced pharmacologically enables polysynaptic activation of NK1R^{+} lamina I neurons by LT inputs.

(B) *In vitro* spinal cord preparation at 4x magnification. Scale bar = 500 μm.

(C) Recorded lamina I NK1R^{+} neuron labeled by fluorescent SP-TMR and filled with Alexa-488. IR-DIC shows same neuron with patch pipette. Scale bar = 100 μm.

(D) Characterization of afferent inputs to NK1R^{+} lamina I neurons in control conditions (top left traces) and after pharmacological disinhibition (10 μm bicuculline, 300 nM

strychnine) (top right traces). In WT slices, dorsal root stimulation at Aδ and C intensities evokes monosynaptic EPSCs in $NK1R^+$ lamina I neurons. With pharmacological disinhibition, low intensity dorsal root stimulation generates Aβ and Aδ polysynaptic EPSCs in $NK1R^+$ lamina I neurons. In VGLUT3 KO slices, Aδ and C stimulation generates monosynaptic events in $NK1R^+$ lamina I neurons (bottom left traces). Under pharmacological disinhibition, low intensity dorsal root stimulation fails to generate EPSCs in $NK1R^+$ lamina I neurons (bottom right traces).

(E) Percent increase in A-fiber-evoked EPSCs in $NK1R^+$ lamina I neurons. Data are normalized to EPSCs measured before disinhibition. n = 7 (WT) and 8 (VGLUT3 KO) total cells from the same number of mice. Mann-Whitney test, *$p<0.05$.

Figure 5. Activation of $VGLUT3^+$ Dorsal Horn Neurons Produces Mechanical Allodynia and Reveals a Polysynaptic Mechanical Allodynia Circuit.

(A) Schematic of the $VGLUT3^{Cre}$ dorsal horn unilaterally injected at P10 with the Cre-dependent excitatory DREADDs virus (AAV8 hSyn-DIO- hM3Dq-mCherry).

(B) Lamina III, but not PKCγ (arrowheads) or DRG neurons express hM3Dq-mCherry. Scale bars = 100 μm except for inset (20 μm) and whole spinal cord (400 μm).

(C) Recording electrode filled with Alexa-488 targets a lamina III neuron expressing hM3Dq-mCherry. Second electrode used to puff on the specific hM3Dq ligand CNO can be seen in DIC picture. Scale bar = 50 μm.

(D) Direct application of 3 mM CNO to an hM3Dq-mCherry expressing neuron generates an inward current in voltage-clamp and series of action potentials in current-clamp.

CNO applied to a cell lacking hM3Dq-mCherry does not elicit a change in membrane potential (bottom trace).

(E) PWTs for VGLUT3^{Cre} and VGLUT3$^{fl/fl}$;VGLUT3^{Cre} mice expressing hM3Dq-mCherry were normal at baseline. After CNO (5 mg/kg) injection, only PWTs of VGLUT3^{Cre} mice dropped dramatically. Hargreaves' withdrawal latencies were unchanged for the two mouse lines (both tests n=7 and n=10 respectively).

(F) After CNO (5 mg/kg) injection, hM3Dq-expressing VGLUT3^{Cre} mice show lifting, fluttering and guarding of the ipsilateral hindpaw. In contrast, hM3Dq-expressing VGLUT3$^{fl/fl}$;VGLUT3^{Cre} mice rarely exhibit the behaviors.

(G) Quantification of c-Fos^{+} cells in laminae I-III and laminae IV-VI of VGLUT3^{Cre} (labeled WT) and VGLUT3$^{fl/fl}$;VGLUT3^{Cre} (labeled KO) mice expressing hM3Dq-mCherry. Hatched bars indicate number of c-Fos^{+} cells that also express mCherry for each condition.

(H) Induction of c-Fos cells in laminae I-III neurons of VGLUT3^{Cre}, but not VGLUT3$^{fl/fl}$;VGLUT3^{Cre} mice (both expressing hM3Dq-mCherry) after CNO injection followed by mechanical stimulation. Scale bars = 100 μm.

(I) Co-staining of c-Fos with PKCγ (21%), calretinin (28%) and Pax2 (14%) neurons in laminae I-III of VGLUT3^{Cre} mice expressing hM3Dq-mCherry after CNO injection followed by mechanical stimulation. Nearly half (48%) of the mCherry^{+} cells were also c-Fos^{+}. Scale bars = 50 μm.

Data are mean ± SEM. *$p<0.05$, **$p \leq 0.01$, ***$p \leq 0.001$.

Figure 6. Characterization of VGLUT3^{+} Neurons and Primary Afferent Input.

(A) Lsl-tdTom;VGLUT3^{Cre} neurons were recorded using transverse spinal cord slices with the dorsal root and DRG still attached. Cells were filled with Alexa-488 and biotin for post-hoc reconstruction. Scale bars = 200 μm (upper left) and 50 μm.

(B) Example traces of tonic, phasic and single firing patterns recorded in tomato^{+} neurons.

(C) The tomato^{+} neurons receive monosynaptic or polysynaptic Aβ inputs.

(D) Incidence of firing patterns and afferent inputs of tomato^{+} neurons.

(E) Morphology of lamina III tomato^{+} neurons. Scale bar = 50 μm.

Figure 7. Activation of Calretinin^{+} Neurons Produces Mechanical Allodynia.

(A) Schematic of the CR^{Cre} dorsal horn unilaterally injected with the hM3Dq-mCherry virus.

(B) The mCherry localizes exclusively to the dorsal region of lamina II$_i$ (arrow), and does not co-localize with PKCγ (arrowhead). Scale bars = 100 μm (left) and 20 μm (right).

(C) In lsl-tdTom;CR^{Cre} mice, tomato is expressed by neurons throughout lamina II$_i$ and co-stains almost completely with calretinin, but very little with PKCγ. Scale bars = 100 μm (left) and 20 μm (right).

(D) PWTs of CR^{Cre} mice expressing hM3Dq-mCherry were normal at baseline, but dropped dramatically after injection of CNO (5 mg/kg). Hargreaves' withdrawal latencies were unaffected (n=8 for both tests).

(E) After CNO (5 mg/kg) injection, CR^{Cre} mice expressing hM3Dq-mCherry demonstrate lifting, fluttering and guarding of the ipsilateral paw.

(F) Representative images and schematics of c-Fos in the dorsal horn of CR^{Cre} mice expressing hM3Dq-mCherry after CNO only (top) or CNO followed by mechanical stimulation (bottom). Scale bars = 100 μm.

(G) Quantification of c-Fos^+ neurons in laminae I-II and laminae III-IV after CNO injection with or without mechanical stimulation, mechanical stimulation only or saline injection only.

(H) c-Fos^+ neurons in laminae I-II induced by CNO plus mechanical stimulation co-stain with calretinin (17%) and Pax2 (35%), but much less with PKCγ (1%). Nearly half (44%) of the $mCherry^+$ cells co-localized with c-Fos. Scale bars = 50 μm.

Data are mean ± SEM. $^{**}p \leq 0.01$, $^{***}p \leq 0.001$.

Figure 8. Expression of c-Fos in inflammatory and neuropathic pain models reveals multiple microcircuits for mechanical allodynia.

(A) Representative pictures of c-Fos induced by carrageenan injection and with (right) or without (left) mechanical stimulation 24 hours later. Scale bars = 100 μm.

(B) Quantification of c-Fos^+ dorsal horn cells after carrageenan injection and with (green bars) or without (black bars) mechanical stimulation 24 hours later.

(C) c-Fos^+ cells colocalize with calretinin (16%), very few with PKCγ (1%) as well as $tomato^+$ lamina III neurons (16%) and $Pax2^+$ cells (41%). Scale bars = 50 μm.

(D) Representative pictures of c-Fos induced by SNI with (right) or without (left) mechanical stimulation delivered 1 week later. Scale bars = 100 μm.

(E) Quantification of c-Fos^+ dorsal horn cells after SNI with (green bars) or without (black bars) mechanical stimulation delivered 1 week later.

(F) c-Fos co-localizes with cells expressing calretinin (7%), PKCγ (6%), tomato (11%) and Pax2 (29%). Scale bars = 50 μm.

(G) Schematic diagram of the circuit for mechanical allodynia. Transient VGLUT3 cells located in lamina III transmit the input from myelinated fibers to the more dorsal neural network underlying mechanical hypersensitivity. Neighboring cells in lamina III receive input from transient VGLUT3 neurons and relay the signal to lamina II cells including $PKC\gamma^+$ and $calretinin^+$ excitatory interneurons that act to refine the excitability of the circuit. Vertical cells in lamina II_o, which receive input from transient VGLUT3 cells and lamina II cells, integrate the signal and send an output to the nociceptive $NK1R^+$ lamina I projection neurons. In persistent pain induced by nerve injury, the "gate" that controls PKCγ is opened resulting in activation of the VGLUT3-PKCγ-calretinin-vertical cell-NK1R pathway (red dotted line). During inflammation, the "gate" that controls calretinin neurons is opened resulting in the activation of the VGLUT3-calretinin-vertical cell-NK1R pathway (blue dotted line). V3: transient VGLUT3; SOM: somatostatin; CR: calretinin; Inh: inhibitory interneurons; Dyn: dynorphin; V: vertical; NK1R: neurokinin 1 receptor.

Data are mean ± SEM. *$p<0.05$, ***$p \leq 0.001$.

REFERENCES

Agarwal, N., Offermanns, S., and Kuner, R. (2004). Conditional gene deletion in primary nociceptive neurons of trigeminal ganglia and dorsal root ganglia. Genesis *38*, 122-129.

Baba, H., Doubell, T.P., Moore, K.A., and Woolf, C.J. (2000). Silent NMDA receptor-mediated synapses are developmentally regulated in the dorsal horn of the rat spinal cord. J. Neurophysiol. *83*, 955-962.

Baba, H., Ji, R.R., Kohno, T., Moore, K.A., Ataka, T., Wakai, A., Okamoto, M., and Woolf, C.J. (2003). Removal of GABAergic inhibition facilitates polysynaptic A fiber-mediated excitatory transmission to the superficial spinal dorsal horn. Mol. Cell Neurosci. *24*, 818-830.

Braz, J., Solorzano, C., Wang, X., and Basbaum, A.I. (2014). Transmitting Pain and Itch Messages: A Contemporary View of the Spinal Cord Circuits that Generate Gate Control. Neuron *82*, 522-536.

Braz, J.M., Rico, B., and Basbaum, A.I. (2002). Transneuronal tracing of diverse CNS circuits by Cre-mediated induction of wheat germ agglutinin in transgenic mice. Proc. Natl. Acad. Sci. *99*, 15148-15153.

Craig, A.D. (2003). Pain mechanisms: labeled lines versus convergence in central processing. Ann. Rev. Neurosci. *26*, 1-30.

Delfini, M.C., Mantilleri, A., Gaillard, S., Hao, J., Reynders, A., Malapert, P., Alonso, S., Francois, A., Barrere, C., Seal, R.*, et al.* (2013). TAFA4, a chemokine-like protein, modulates injury-induced mechanical and chemical pain hypersensitivity in mice. Cell Rep. *5*, 378-388.

Duan, B., Cheng, L., Bourane, S., Britz, O., Padilla, C., Garcia-Campmany, L., Krashes, M., Knowlton, W., Velasquez, T., Ren, X.*, et al.* (2014). Identification of spinal circuits transmitting and gating mechanical pain. Cell *159*, 1417-1432.

Fitzgerald, M. (2005). The development of nociceptive circuits. Nat. Rev. Neurosci. *6*, 507-520.

Gao, Y.J., and Ji, R.R. (2010). Light touch induces ERK activation in superficial dorsal horn neurons after inflammation: involvement of spinal astrocytes and JNK signaling in touch-evoked central sensitization and mechanical allodynia. J. Neurochem. *115*, 505-514.

Grimes, W.N., Seal, R.P., Oesch, N., Edwards, R.H., and Diamond, J.S. (2011). Genetic targeting and physiological features of VGLUT3+ amacrine cells. Vis. Neurosci. *28*, 381-392.

Hafner, M., Wenk, J., Nenci, A., Pasparakis, M., Scharffetter-Kochanek, K., Smyth, N., Peters, T., Kess, D., Holtkotter, O., Shephard, P.*, et al.* (2004). Keratin 14 Cre transgenic mice authenticate keratin 14 as an oocyte-expressed protein. Genesis *38*, 176-181.

Hasegawa, H., Abbott, S., Han, B.X., Qi, Y., and Wang, F. (2007). Analyzing somatosensory axon projections with the sensory neuron-specific Advillin gene. J. Neurosci. *27*, 14404-14414.

Kato, G., Kawasaki, Y., Koga, K., Uta, D., Kosugi, M., Yasaka, T., Yoshimura, M., Ji, R.R., and Strassman, A.M. (2009). Organization of intralaminar and translaminar neuronal connectivity in the superficial spinal dorsal horn. J. Neurosci. *29*, 5088-5099.

Kuner, R. (2010). Central mechanisms of pathological pain. Nat. Med. *16*, 1258-1266.

Li, L., Rutlin, M., Abraira, V.E., Cassidy, C., Kus, L., Gong, S., Jankowski, M.P., Luo, W., Heintz, N., Koerber, H.R.*, et al.* (2011). The functional organization of cutaneous low-threshold mechanosensory neurons. Cell *147*, 1615-1627.

Li, P., and Zhuo, M. (1998). Silent glutamatergic synapses and nociception in mammalian spinal cord. Nature *393*, 695-698.

Liljencrantz, J., Bjornsdotter, M., Morrison, I., Bergstrand, S., Ceko, M., Seminowicz, D.A., Cole, J., Bushnell, M.C., and Olausson, H. (2013). Altered C-tactile processing in human dynamic tactile allodynia. Pain *154*, 227-234.

Loken, L.S., Wessberg, J., Morrison, I., McGlone, F., and Olausson, H. (2009). Coding of pleasant touch by unmyelinated afferents in humans. Nat. Neurosci. *12*, 547-548.

Lou, S., Duan, B., Vong, L., Lowell, B.B., and Ma, Q. (2013). Runx1 controls terminal morphology and mechanosensitivity of VGLUT3-expressing C-mechanoreceptors. J. Neurosci. *33*, 870-882.

Lu, Y., Dong, H., Gao, Y., Gong, Y., Ren, Y., Gu, N., Zhou, S., Xia, N., Sun, Y.Y., Ji, R.R.*, et al.* (2013). A feed-forward spinal cord glycinergic neural circuit gates mechanical allodynia. J. Clin. Invest. *123*, 4050-4062.

Lu, Y., and Perl, E.R. (2005). Modular organization of excitatory circuits between neurons of the spinal superficial dorsal horn (laminae I and II). J. Neurosci. *25*, 3900-3907.

Madisen, L., Zwingman, T.A., Sunkin, S.M., Oh, S.W., Zariwala, H.A., Gu, H., Ng, L.L., Palmiter, R.D., Hawrylycz, M.J., Jones, A.R.*, et al.* (2010). A robust and high-throughput Cre reporting and characterization system for the whole mouse brain. Nat. Neurosci. *13*, 133-140.

Malmberg, A.B., Chen, C., Tonegawa, S., and Basbaum, A.I. (1997). Preserved acute pain and reduced neuropathic pain in mice lacking PKCgamma. Science *278*, 279-283.

Melzack, R., and Wall, P.D. (1965). Pain mechanisms: a new theory. Science *150*, 971-979.

Miraucourt, L.S., Dallel, R., and Voisin, D.L. (2007). Glycine inhibitory dysfunction turns touch into pain through PKCgamma interneurons. PLoS One *2*, e1116.

Nagi, S.S., Rubin, T.K., Chelvanayagam, D.K., Macefield, V.G., and Mahns, D.A. (2011). Allodynia mediated by C-tactile afferents in human hairy skin. J. Neurophysiol. *589*, 4065-4075.

Peirs, C., Patil, S., Bouali-Benazzouz, R., Artola, A., Landry, M., and Dallel, R. (2014). Protein kinase C gamma interneurons in the rat medullary dorsal horn: distribution and synaptic inputs to these neurons, and subcellular localization of the enzyme. J. Comp. Neurol. *522*, 393-413.

Polgar, E., Campbell, A.D., MacIntyre, L.M., Watanabe, M., and Todd, A.J. (2007a). Phosphorylation of ERK in neurokinin 1 receptor-expressing neurons in laminae III and IV of the rat spinal dorsal horn following noxious stimulation. Mol. Pain *3*, 4.

Polgar, E., Fowler, J.H., McGill, M.M., and Todd, A.J. (1999). The types of neuron which contain protein kinase C gamma in rat spinal cord. Brain Res. *833*, 71-80.

Polgar, E., Thomson, S., Maxwell, D.J., Al-Khater, K., and Todd, A.J. (2007b). A population of large neurons in laminae III and IV of the rat spinal cord that have long dorsal dendrites and lack the neurokinin 1 receptor. Eur. J. Neurosci. *26*, 1587-1598.

Prescott, S.A., Ma, Q., and De Koninck, Y. (2014). Normal and abnormal coding of somatosensory stimuli causing pain. Nat. Neurosci *17*, 183-191.

Ross, S.E., Mardinly, A.R., McCord, A.E., Zurawski, J., Cohen, S., Jung, C., Hu, L., Mok, S.I., Shah, A., Savner, E.M.*, et al.* (2010). Loss of inhibitory interneurons in the dorsal spinal cord and elevated itch in Bhlhb5 mutant mice. Neuron *65*, 886-898.

Scherrer, G., Low, S.A., Wang, X., Zhang, J., Yamanaka, H., Urban, R., Solorzano, C., Harper, B., Hnasko, T.S., Edwards, R.H.*, et al.* (2010). VGLUT2 expression in primary afferent neurons is essential for normal acute pain and injury-induced heat hypersensitivity. Proc. Natl. Acad. Sci. *107*, 22296-22301.

Schneider, S.P. (2008). Local circuit connections between hamster laminae III and IV dorsal horn neurons. J. Neurophysiol. *99*, 1306-1318.

Seal, R.P., Akil, O., Yi, E., Weber, C.M., Grant, L., Yoo, J., Clause, A., Kandler, K., Noebels, J.L., Glowatzki, E.*, et al.* (2008). Sensorineural deafness and seizures in mice lacking vesicular glutamate transporter 3. Neuron *57*, 263-275.

Seal, R.P., Wang, X., Guan, Y., Raja, S.N., Woodbury, C.J., Basbaum, A.I., and Edwards, R.H. (2009). Injury-induced mechanical hypersensitivity requires C-low threshold mechanoreceptors. Nature *462*, 651-655.

Sieber, M.A., Storm, R., Martinez-de-la-Torre, M., Muller, T., Wende, H., Reuter, K., Vasyutina, E., and Birchmeier, C. (2007). Lbx1 acts as a selector gene in the fate determination of somatosensory and viscerosensory relay neurons in the hindbrain. J. Neurosci. *27*, 4902-4909.

Todd, A.J. (2010). Neuronal circuitry for pain processing in the dorsal horn. Nat. Rev. Neurosci. *11*, 823-836.

Torsney, C., and MacDermott, A.B. (2006). Disinhibition opens the gate to pathological pain signaling in superficial neurokinin 1 receptor-expressing neurons in rat spinal cord. J. Neurosci. *26*, 1833-1843.

Varrassi, G., Muller-Schwefe, G., Pergolizzi, J., Oronska, A., Morlion, B., Mavrocordatos, P., Margarit, C., Mangas, C., Jaksch, W., Huygen, F.*, et al.* (2010). Pharmacological treatment of chronic pain - the need for CHANGE. Curr Med Res Opin *26*, 1231-1245.

von Hehn, C.A., Baron, R., and Woolf, C.J. (2012). Deconstructing the neuropathic pain phenotype to reveal neural mechanisms. Neuron *73*, 638-652.

Vrontou, S., Wong, A.M., Rau, K.K., Koerber, H.R., and Anderson, D.J. (2013). Genetic identification of C fibres that detect massage-like stroking of hairy skin in vivo. Nature *493*, 669-673.

Wang, X., Zhang, J., Eberhart, D., Urban, R., Meda, K., Solorzano, C., Yamanaka, H., Rice, D., and Basbaum, A.I. (2013). Excitatory superficial dorsal horn interneurons are functionally heterogeneous and required for the full behavioral expression of pain and itch. Neuron *78*, 312-324.

Witschi, R., Johansson, T., Morscher, G., Scheurer, L., Deschamps, J., and Zeilhofer, H.U. (2010). Hoxb8-Cre mice: A tool for brain-sparing conditional gene deletion. Genesis *48*, 596-602.

Xu, Y., Lopes, C., Wende, H., Guo, Z., Cheng, L., Birchmeier, C., and Ma, Q. (2013). Ontogeny of excitatory spinal neurons processing distinct somatic sensory modalities. J. Neurosci. *33*, 14738-14748.

Yasaka, T., Tiong, S.Y., Polgar, E., Watanabe, M., Kumamoto, E., Riddell, J.S., and Todd, A.J. (2014). A putative relay circuit providing low-threshold mechanoreceptive input to lamina I projection neurons via vertical cells in lamina II of the rat dorsal horn. Mol. Pain *10*, 3.

Zeilhofer, H.U., Wildner, H., and Yevenes, G.E. (2012). Fast synaptic inhibition in spinal sensory processing and pain control. Physiol. Rev. *92*, 193-235.

Zhao, C., Leitges, M., and Gereau, R.W.t. (2011). Isozyme-specific effects of protein kinase C in pain modulation. Anesthesiology *115*, 1261-1270.

Zou, W., Song, Z., Guo, Q., Liu, C., Zhang, Z., and Zhang, Y. (2011). Intrathecal lentiviral-mediated RNA interference targeting PKCgamma attenuates chronic constriction injury-induced neuropathic pain in rats. Human Gene Ther. *22*, 465-475.

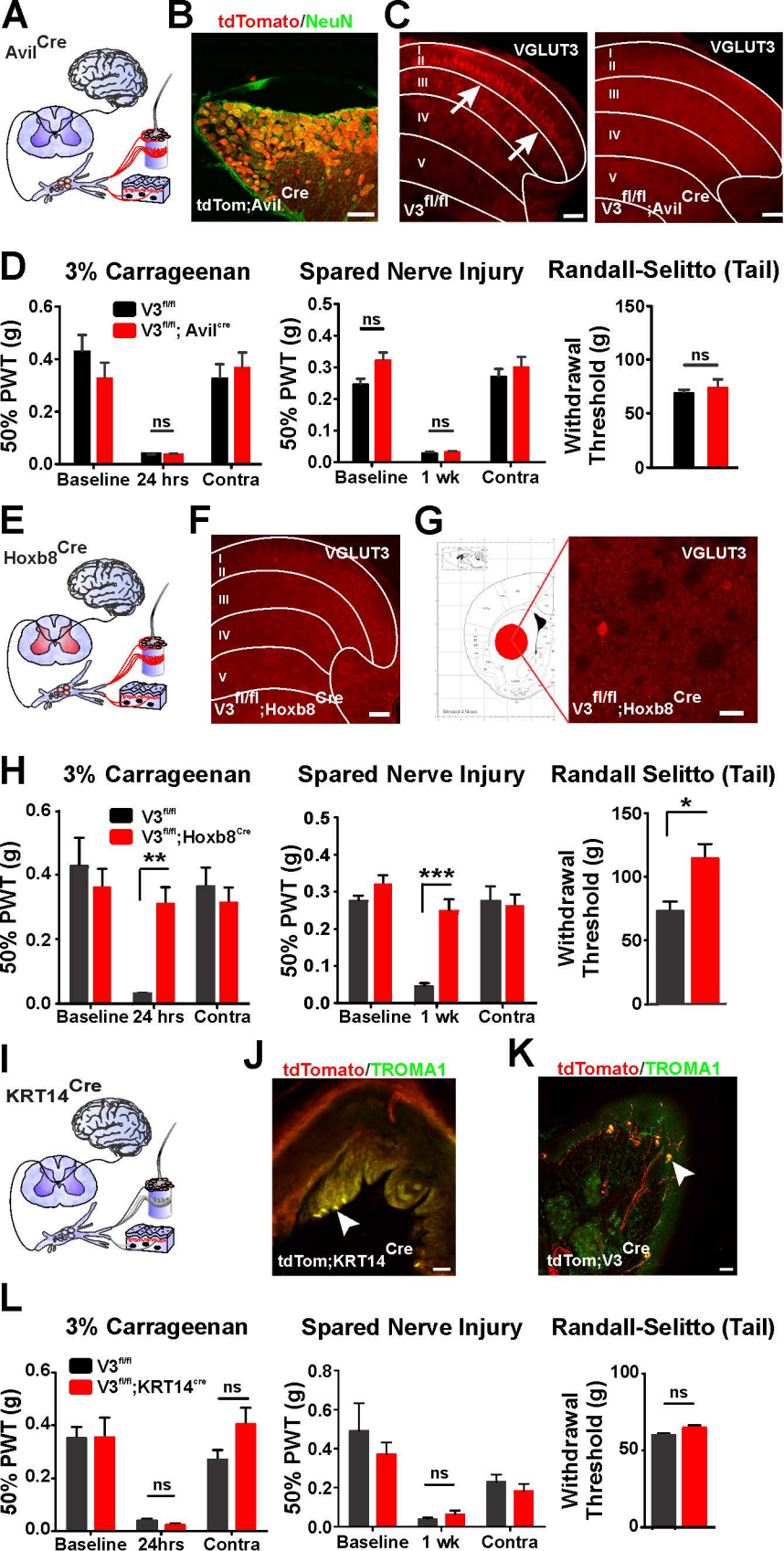
A
Avil Cre
B
tdTomato/NeuN
tdTom;Avil Cre
C
VGLUT3
V3 fl/fl
V3 fl/fl ;Avil Cre
D
3% Carrageenan
Spared Nerve Injury
Randall-Selitto (Tail)
V3 fl/fl
V3 fl/fl; Avil cre
50% PWT (g)
Withdrawal Threshold (g)
ns
Baseline 24 hrs Contra
Baseline 1 wk Contra
E
Hoxb8 Cre
F
VGLUT3
V3 fl/fl ;Hoxb8 Cre
G
VGLUT3
V3 fl/fl ;Hoxb8 Cre
H
3% Carrageenan
Spared Nerve Injury
Randall Selitto (Tail)
V3 fl/fl
V3 fl/fl;Hoxb8 Cre
**
***
*
Baseline 24 hrs Contra
Baseline 1 wk Contra
I
KRT14 Cre
J
tdTomato/TROMA1
tdTom;KRT14 Cre
K
tdTomato/TROMA1
tdTom;V3 Cre
L
3% Carrageenan
Spared Nerve Injury
Randall-Selitto (Tail)
V3 fl/fl
V3 fl/fl;KRT14 cre
ns
Baseline 24hrs Contra
Baseline 1 wk Contra

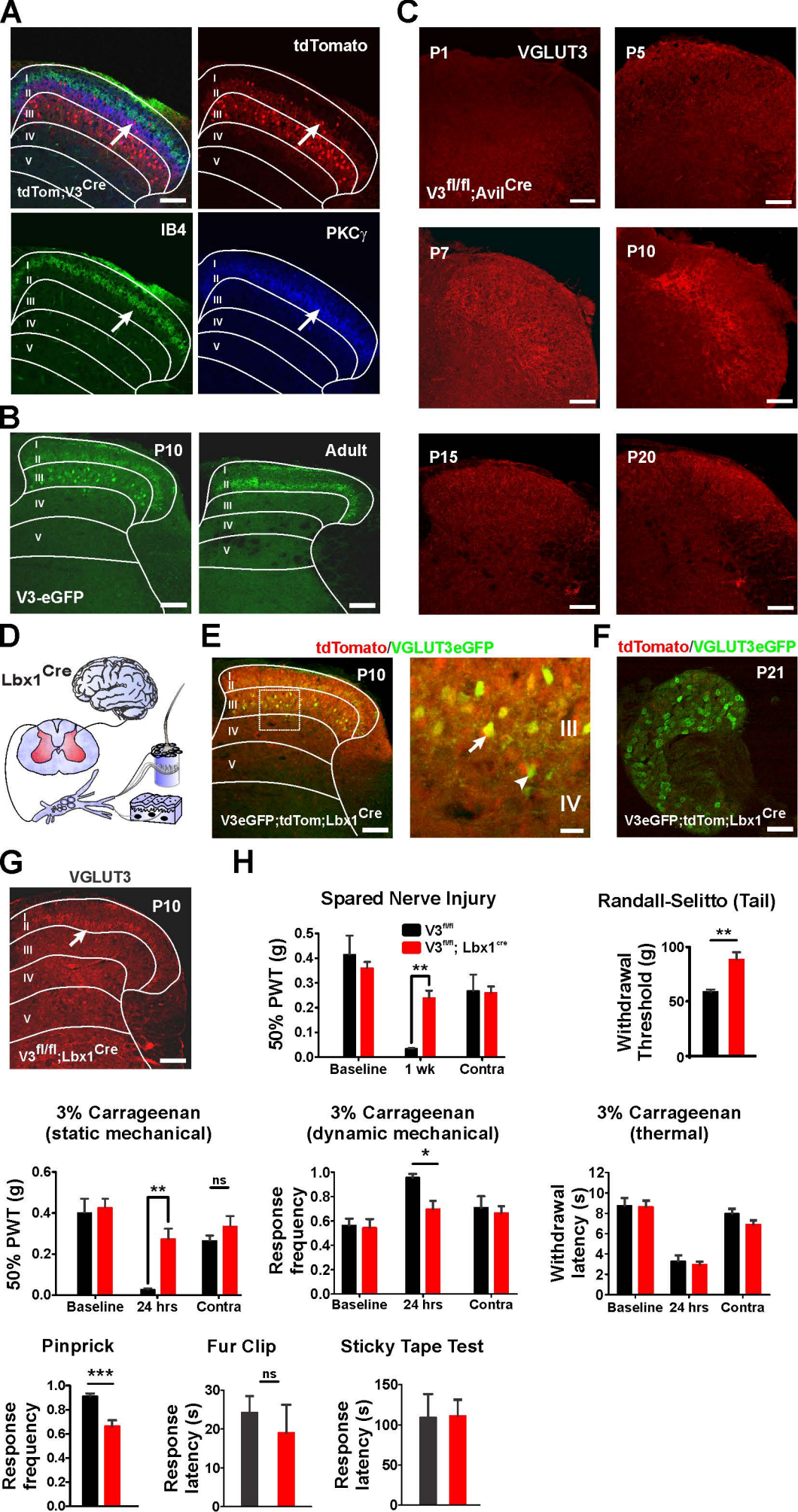
A
tdTomato
tdTom;V3Cre
IB4
PKCγ
B
P10
Adult
V3-eGFP
C
P1
VGLUT3
V3fl/fl;AvilCre
P5
P7
P10
P15
P20
D
Lbx1Cre
E
tdTomato/VGLUT3eGFP
P10
V3eGFP;tdTom;Lbx1Cre
III
IV
F
tdTomato/VGLUT3eGFP
P21
V3eGFP;tdTom;Lbx1Cre
G
VGLUT3
P10
V3fl/fl;Lbx1Cre
H
Spared Nerve Injury
V3fl/fl
V3fl/fl; Lbx1cre
50% PWT (g)
Baseline
1 wk
Contra
Randall-Selitto (Tail)
Withdrawal Threshold (g)
3% Carrageenan (static mechanical)
50% PWT (g)
ns
Baseline
24 hrs
Contra
3% Carrageenan (dynamic mechanical)
Response frequency
3% Carrageenan (thermal)
Withdrawal latency (s)
Pinprick
Response frequency
Fur Clip
Response latency (s)
Sticky Tape Test
Response latency (s)

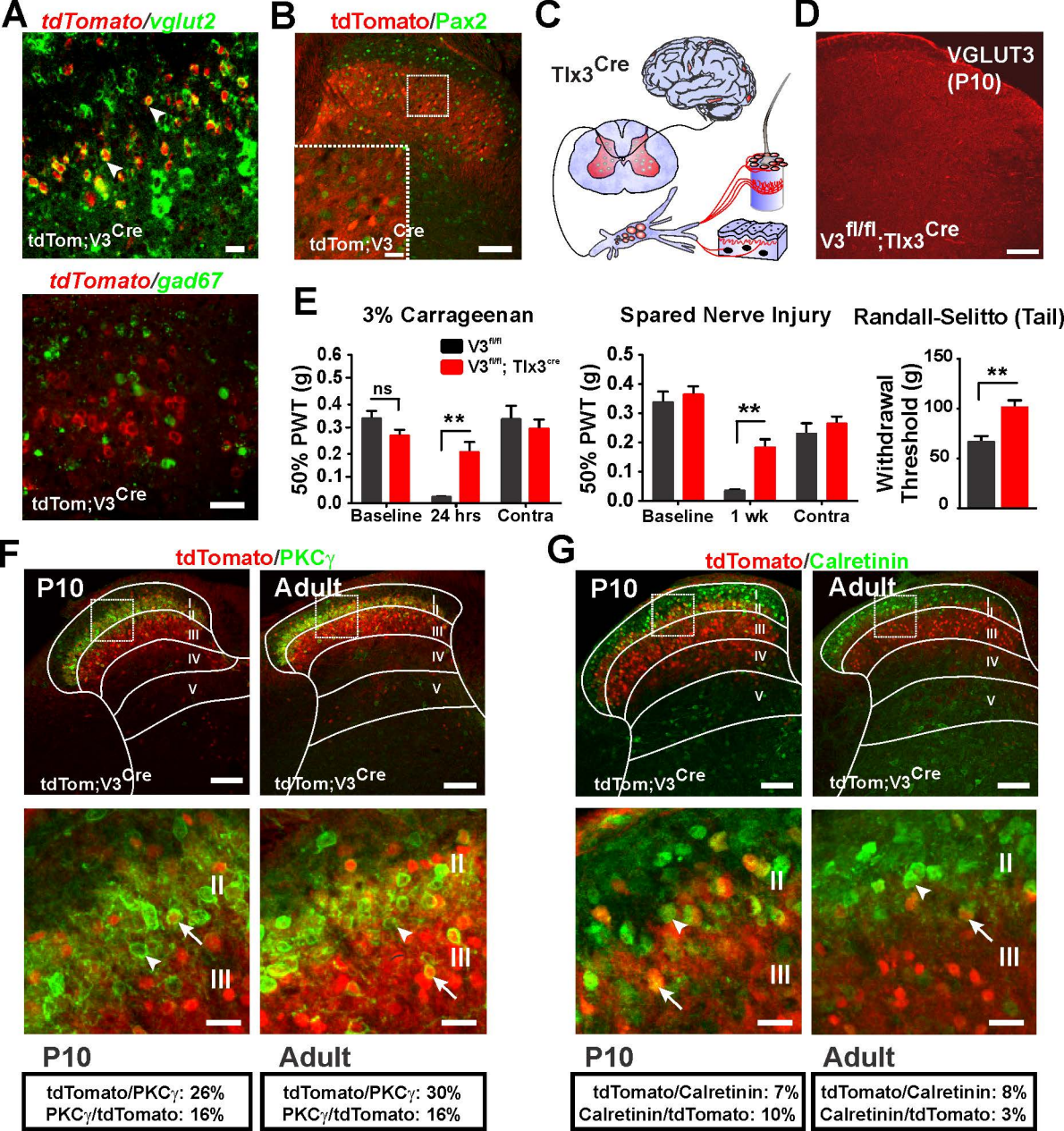
A
tdTomato/vglut2
tdTom;V3Cre
tdTomato/gad67
tdTom;V3Cre
B
tdTomato/Pax2
tdTom;V3Cre
C
Tlx3Cre
D
VGLUT3
(P10)
V3fl/fl;Tlx3Cre
E
3% Carrageenan
V3fl/fl
V3fl/fl; Tlx3cre
50% PWT (g)
ns
**
Baseline
24 hrs
Contra
Spared Nerve Injury
50% PWT (g)
**
Baseline
1 wk
Contra
Randall-Selitto (Tail)
Withdrawal Threshold (g)
**
F
tdTomato/PKCγ
P10
Adult
tdTom;V3Cre
tdTom;V3Cre
II
III
IV
V
P10
tdTomato/PKCγ: 26%
PKCγ/tdTomato: 16%
Adult
tdTomato/PKCγ: 30%
PKCγ/tdTomato: 16%
G
tdTomato/Calretinin
P10
Adult
tdTom;V3Cre
tdTom;V3Cre
P10
tdTomato/Calretinin: 7%
Calretinin/tdTomato: 10%
Adult
tdTomato/Calretinin: 8%
Calretinin/tdTomato: 3%

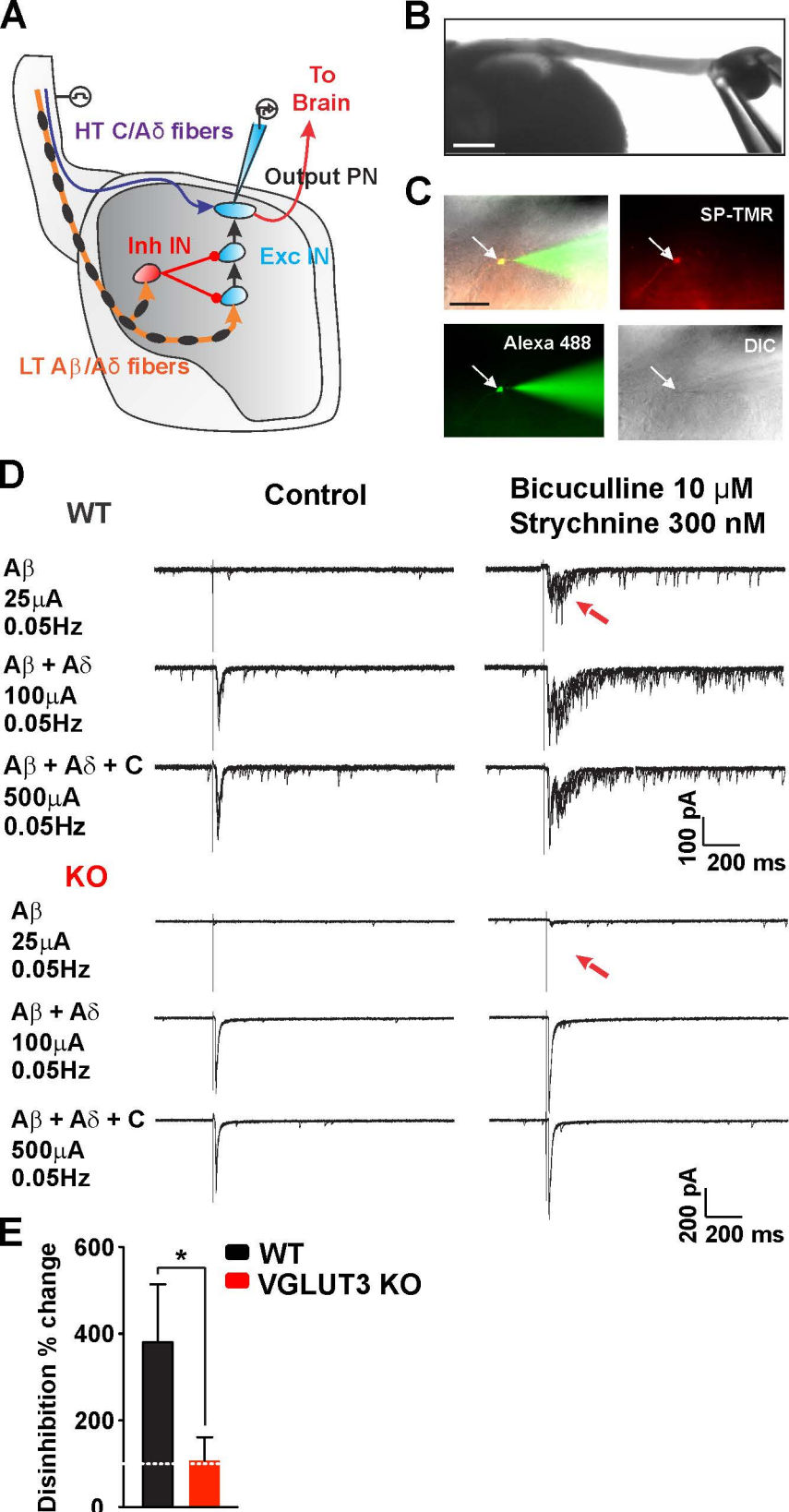
A
To
Brain
HT C/Aδ fibers
Output PN
Inh IN
Exc IN
LT Aβ/Aδ fibers
B
C
SP-TMR
Alexa 488
DIC
D
WT
Control
Bicuculline 10 μM
Strychnine 300 nM
Aβ
25μA
0.05Hz
Aβ + Aδ
100μA
0.05Hz
Aβ + Aδ + C
500μA
0.05Hz
100 pA
200 ms
KO
Aβ
25μA
0.05Hz
Aβ + Aδ
100μA
0.05Hz
Aβ + Aδ + C
500μA
0.05Hz
200 pA
200 ms
E
Disinhibition % change
600
400
200
0
*
WT
VGLUT3 KO

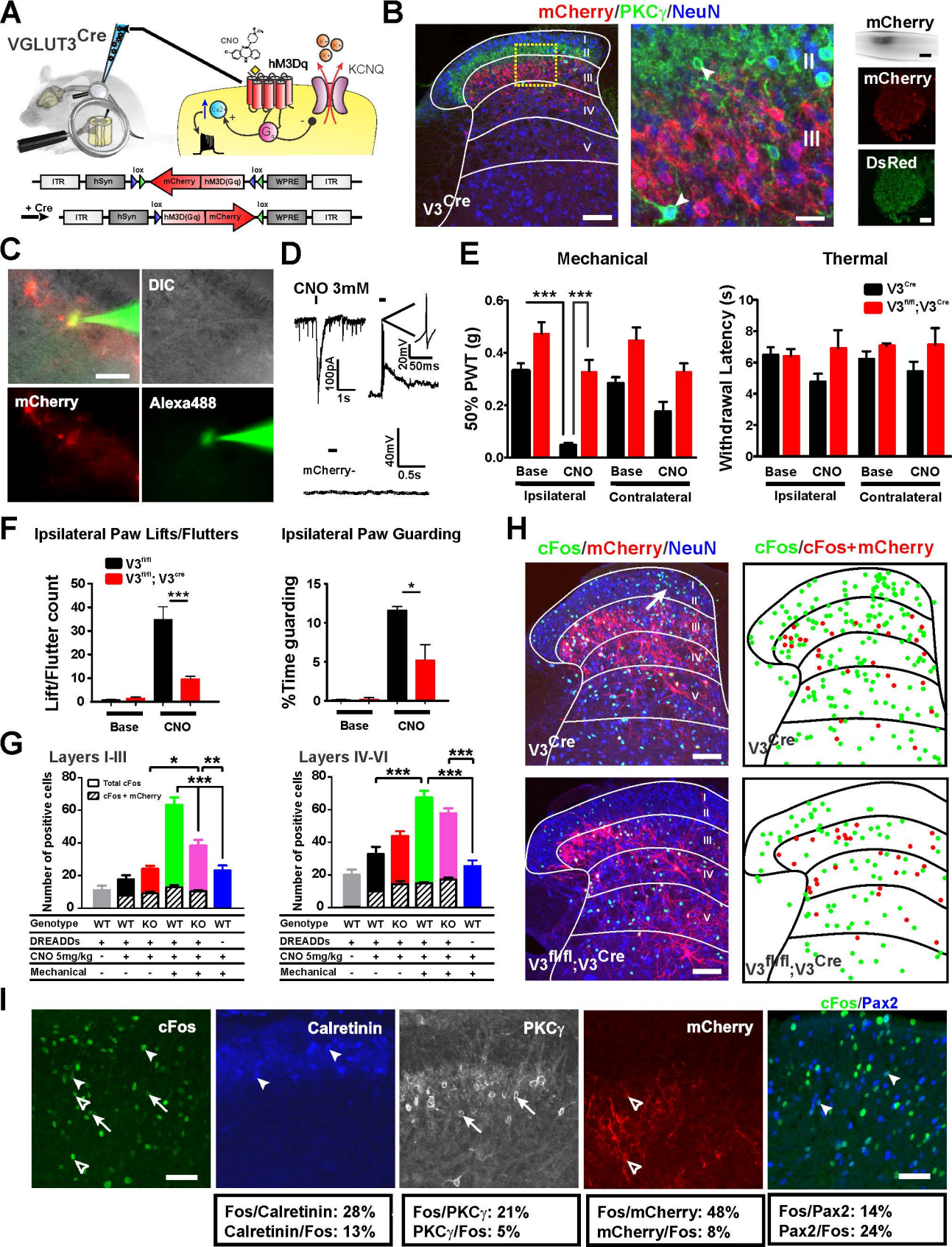
A
VGLUT3Cre
CNO
hM3Dq
KCNQ
ITR
hSyn
lox
mCherry
hM3D(Gq)
WPRE
+ Cre
B
mCherry/PKCγ/NeuN
V3Cre
mCherry
DsRed
C
DIC
mCherry
Alexa488
D
CNO 3mM
100pA
1s
20mV
50ms
mCherry-
40mV
0.5s
E
Mechanical
Thermal
50% PWT (g)
Withdrawal Latency (s)
V3Cre
V3fl/fl;V3Cre
Base
CNO
Ipsilateral
Contralateral
F
Ipsilateral Paw Lifts/Flutters
Ipsilateral Paw Guarding
Lift/Flutter count
%Time guarding
G
Layers I-III
Layers IV-VI
Total cFos
cFos + mCherry
Number of positive cells
Genotype
DREADDs
CNO 5mg/kg
Mechanical
H
cFos/mCherry/NeuN
cFos/cFos+mCherry
I
cFos
Calretinin
PKCγ
mCherry
cFos/Pax2
Fos/Calretinin: 28%
Calretinin/Fos: 13%
Fos/PKCγ: 21%
PKCγ/Fos: 5%
Fos/mCherry: 48%
mCherry/Fos: 8%
Fos/Pax2: 14%
Pax2/Fos: 24%

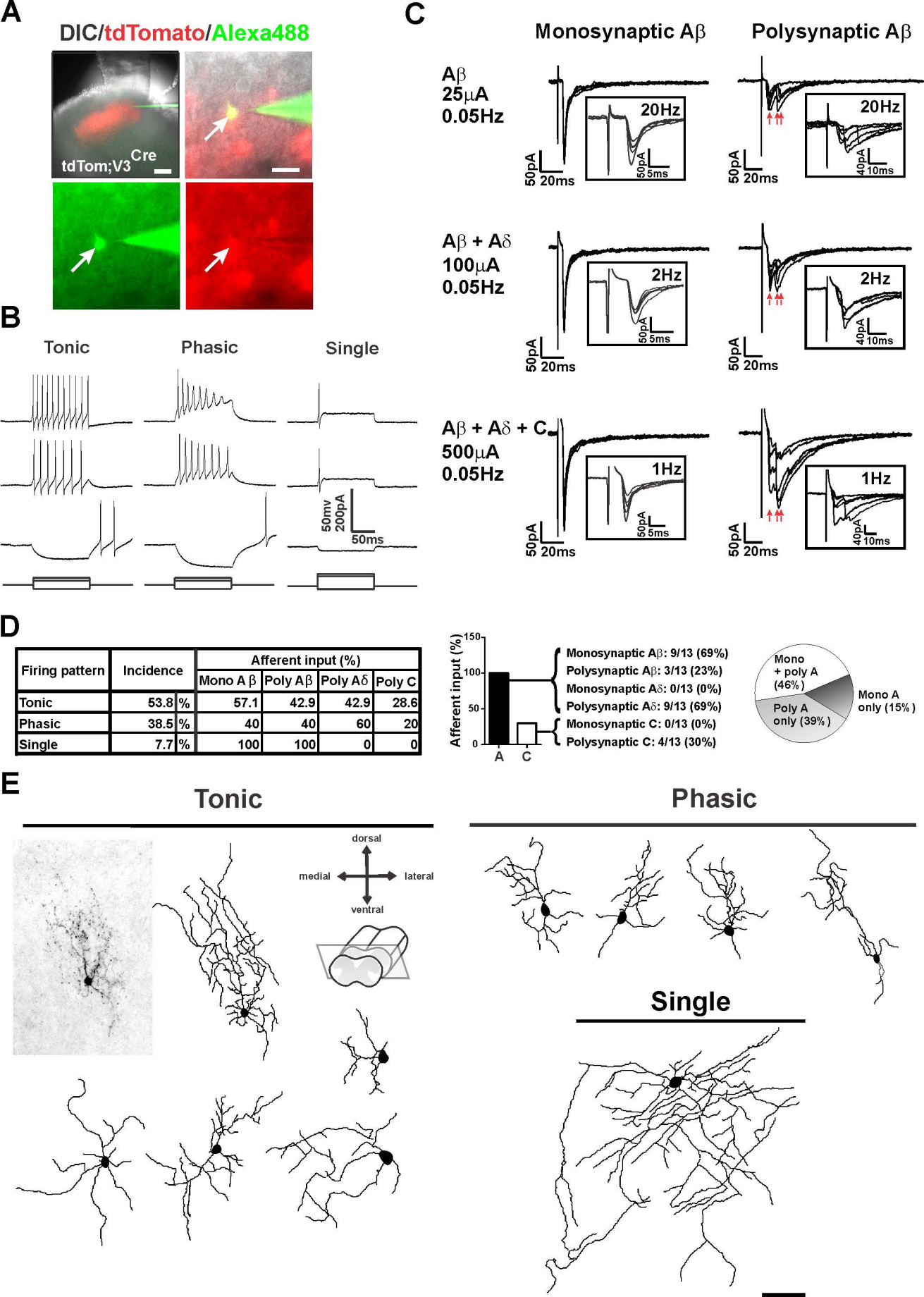

Firing pattern	Incidence		Afferent input (%)			
			Mono A β	Poly Aβ	Poly Aδ	Poly C
Tonic	53.8	%	57.1	42.9	42.9	28.6
Phasic	38.5	%	40	40	60	20
Single	7.7	%	100	100	0	0

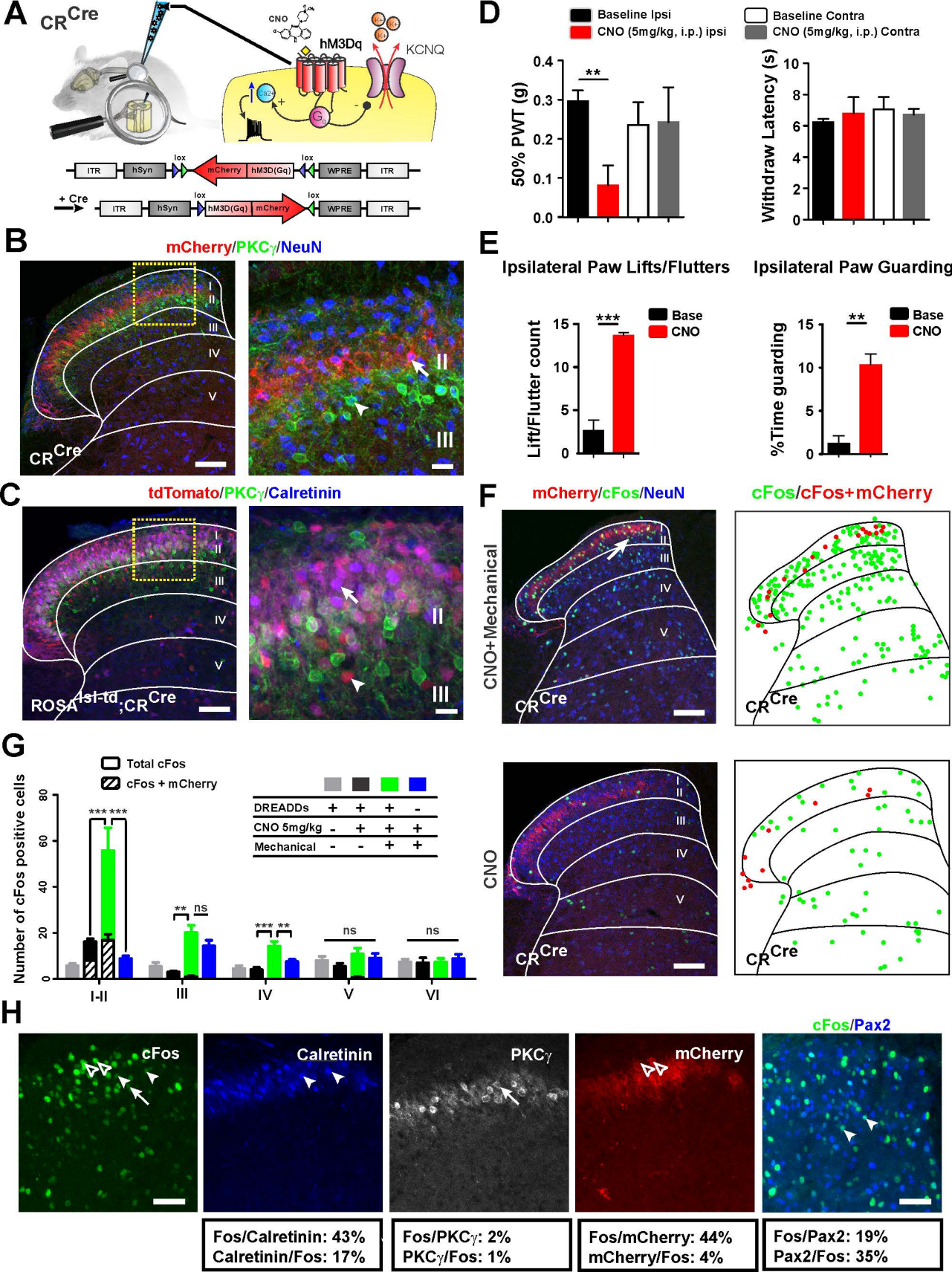
A
CRCre
hM3Dq
KCNQ
CNO
ITR
hSyn
lox
mCherry
hM3D(Gq)
WPRE
+ Cre
B
mCherry/PKCγ/NeuN
CRCre
C
tdTomato/PKCγ/Calretinin
ROSA1sl-td;CRCre
D
Baseline Ipsi
CNO (5mg/kg, i.p.) ipsi
Baseline Contra
CNO (5mg/kg, i.p.) Contra
50% PWT (g)
Withdraw Latency (s)
E
Ipsilateral Paw Lifts/Flutters
Ipsilateral Paw Guarding
Lift/Flutter count
%Time guarding
Base
CNO
F
mCherry/cFos/NeuN
cFos/cFos+mCherry
CNO+Mechanical
CNO
G
Total cFos
cFos + mCherry
Number of cFos positive cells
DREADDs
CNO 5mg/kg
Mechanical
I-II
III
IV
V
VI
ns
H
cFos
Calretinin
PKCγ
mCherry
cFos/Pax2
Fos/Calretinin: 43%
Calretinin/Fos: 17%
Fos/PKCγ: 2%
PKCγ/Fos: 1%
Fos/mCherry: 44%
mCherry/Fos: 4%
Fos/Pax2: 19%
Pax2/Fos: 35%

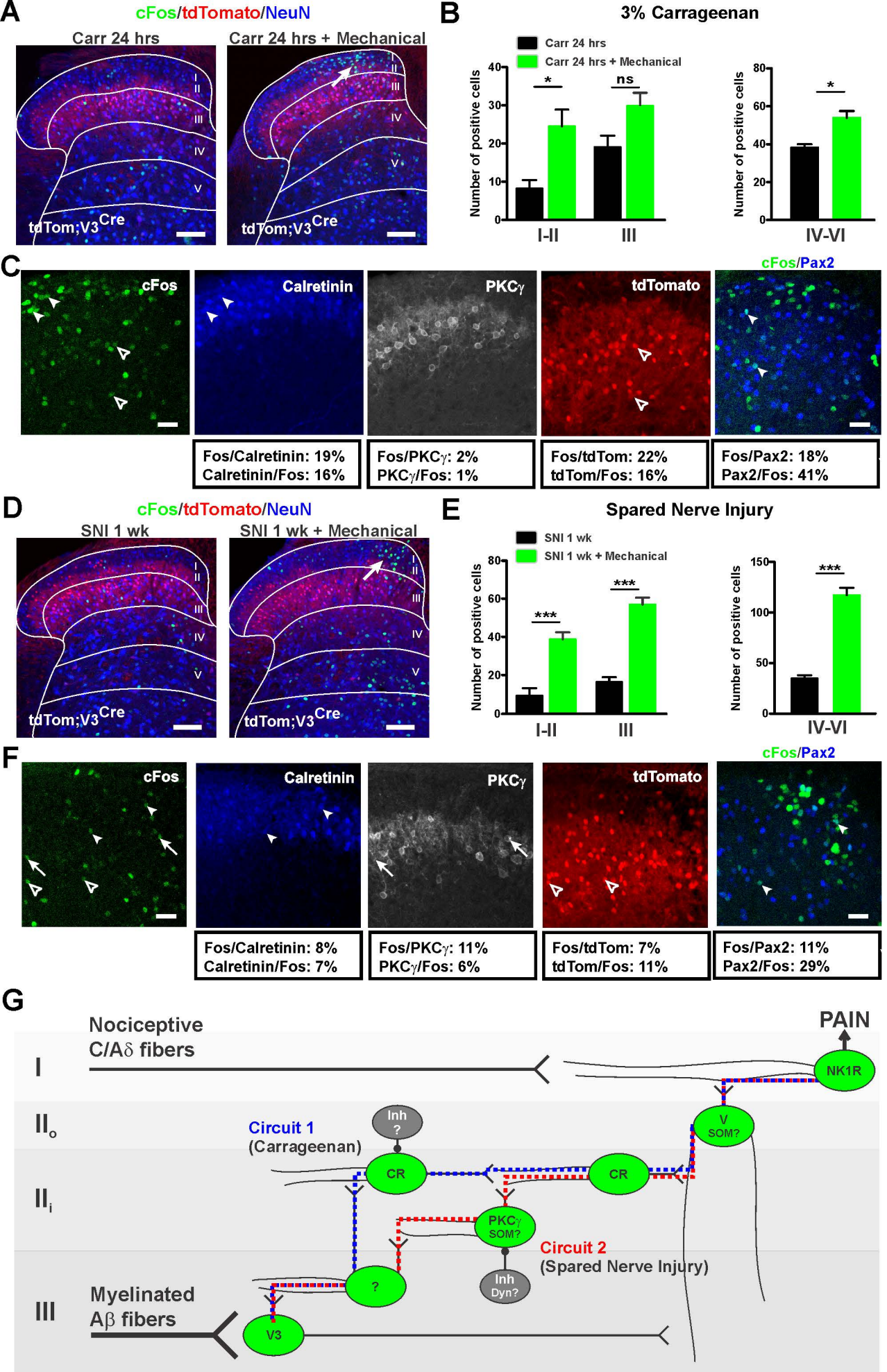
A
cFos/tdTomato/NeuN
Carr 24 hrs
Carr 24 hrs + Mechanical
tdTom;V3Cre
tdTom;V3Cre
B
3% Carrageenan
Carr 24 hrs
Carr 24 hrs + Mechanical
Number of positive cells
*
ns
I-II
III
*
IV-VI
C
cFos
Calretinin
PKCγ
tdTomato
cFos/Pax2
Fos/Calretinin: 19%
Calretinin/Fos: 16%
Fos/PKCγ: 2%
PKCγ/Fos: 1%
Fos/tdTom: 22%
tdTom/Fos: 16%
Fos/Pax2: 18%
Pax2/Fos: 41%
D
cFos/tdTomato/NeuN
SNI 1 wk
SNI 1 wk + Mechanical
tdTom;V3Cre
tdTom;V3Cre
E
Spared Nerve Injury
SNI 1 wk
SNI 1 wk + Mechanical
Number of positive cells
***
***
I-II
III
***
IV-VI
F
cFos
Calretinin
PKCγ
tdTomato
cFos/Pax2
Fos/Calretinin: 8%
Calretinin/Fos: 7%
Fos/PKCγ: 11%
PKCγ/Fos: 6%
Fos/tdTom: 7%
tdTom/Fos: 11%
Fos/Pax2: 11%
Pax2/Fos: 29%
G
Nociceptive
C/Aδ fibers
PAIN
I
NK1R
II o
Circuit 1
(Carrageenan)
Inh
?
V
SOM?
CR
CR
II i
PKCγ
SOM?
Circuit 2
(Spared Nerve Injury)
Inh
Dyn?
?
III
Myelinated
Aβ fibers
V3

SUPPLEMENTAL DATA

SUPPLEMENTAL FIGURES AND LEGENDS

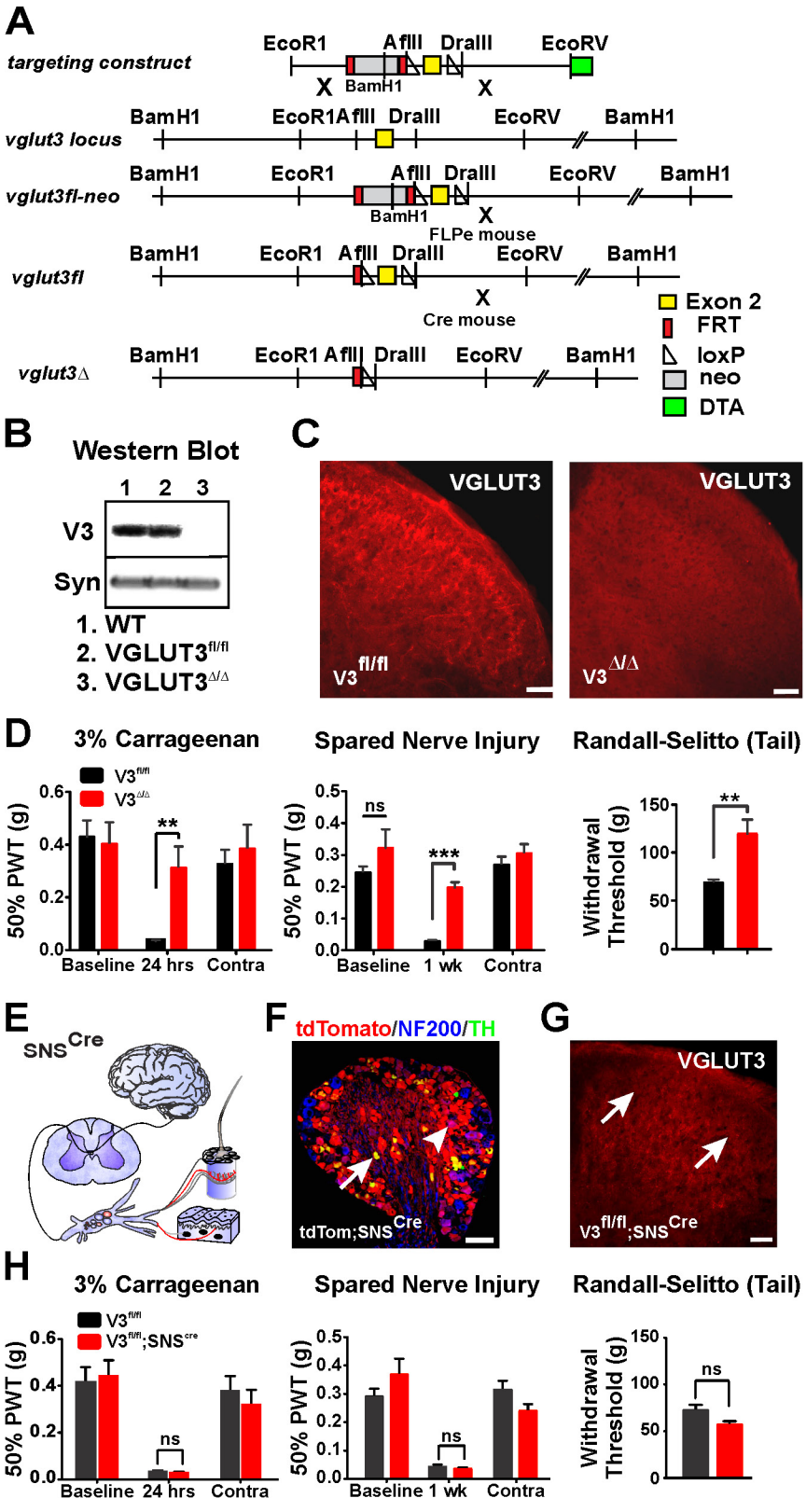
A
targeting construct
EcoR1
AflII
DraIII
EcoRV
X
BamH1
X
vglut3 locus
BamH1
EcoR1
AflII
DraIII
EcoRV
BamH1
vglut3fl-neo
BamH1
EcoR1
AflII
DraIII
EcoRV
BamH1
BamH1
X
FLPe mouse
vglut3fl
BamH1
EcoR1
AflII
DraIII
EcoRV
BamH1
X
Cre mouse
vglut3Δ
BamH1
EcoR1
AflII
DraIII
EcoRV
BamH1
Exon 2
FRT
loxP
neo
DTA
B
Western Blot
1 2 3
V3
Syn
1. WT
2. VGLUT3fl/fl
3. VGLUT3Δ/Δ
C
VGLUT3
V3fl/fl
VGLUT3
V3Δ/Δ
D
3% Carrageenan
Spared Nerve Injury
Randall-Selitto (Tail)
V3fl/fl
V3Δ/Δ
50% PWT (g)
0.6
0.4
0.2
0.0
**
Baseline
24 hrs
Contra
50% PWT (g)
0.5
0.4
0.3
0.2
0.1
0.0
ns
***
Baseline
1 wk
Contra
Withdrawal Threshold (g)
150
100
50
0
**
E
SNSCre
F
tdTomato/NF200/TH
tdTom;SNSCre
G
VGLUT3
V3fl/fl;SNSCre
H
3% Carrageenan
Spared Nerve Injury
Randall-Selitto (Tail)
V3fl/fl
V3fl/fl;SNScre
50% PWT (g)
0.6
0.4
0.2
0.0
ns
Baseline
24 hrs
Contra
50% PWT (g)
0.5
0.4
0.3
0.2
0.1
0.0
ns
Baseline
1 wk
Contra
Withdrawal Threshold (g)
150
100
50
0
ns

Figure S1, Related to Figure 1. Description of VGLUT3$^{fl/fl}$ Mice and conditional deletion of VGLUT3 from primary afferents.

(A) VGLUT3$^{fl/fl}$ targeting construct and *vglut3* gene locus before and after homologous recombination. LoxP sites flank exon 2. FRT sites flank the positive selectable marker, TK-*neomyosin*. Diphtheria toxin A (DTA) is the negative selectable marker.

(B) Western blot of brain tissue homogenate from VGLUT3^{WT}, VGLUT3$^{fl/fl}$ and VGLUT3$^{\Delta/\Delta}$ mice probed for VGLUT3 and for synaptophysin as control.

(C) VGLUT3-IR in spinal cord of adult VGLUT3$^{fl/fl}$ (left) and VGLUT3$^{\Delta/\Delta}$ (right) mice. VGLUT3-IR is absent in the VGLUT3$^{\Delta/\Delta}$ mice.

(D) Paw Withdrawal Thresholds (PWT) in the carrageenan and SNI models are normal in VGLUT3$^{fl/fl}$ mice (n=6 and 4, respectively), but are attenuated in the VGLUT3 $^{\Delta/\Delta}$ mice (n= 8 and 4, respectively). Randall-Selitto thresholds are also significantly higher in VGLUT3 $^{\Delta/\Delta}$ compared to VGLUT3$^{fl/fl}$ mice (n=4 and n=6).

(E) SNS^{Cre} mice express Cre in DRG neurons (all unmyelinated, some myelinated).

(F) In the lsl-tdTom;SNS^{Cre} mice, tomato is present in unmyelinated neurons including C-LTMRs (arrow), and some myelinated afferents (arrowhead).

(G) VGLUT3$^{fl/fl}$;SNS^{Cre} mice lack VGLUT3-IR in lamina II$_i$ (arrows) of the dorsal horn.

(H) Mechanical allodynia is normal in VGLUT3$^{fl/fl}$;SNS^{Cre} mice. PWTs did not differ from VGLUT3$^{fl/fl}$ controls after carrageenan (n=10 and n=8 respectively) or SNI (n=5 and n=4 respectively). Randall-Selitto responses also did not differ (n=8 and n=6 respectively).

All scale bars = 100 μm. Data are Mean ± SEM. **p ≤ 0.01, ***p ≤ 0.001.

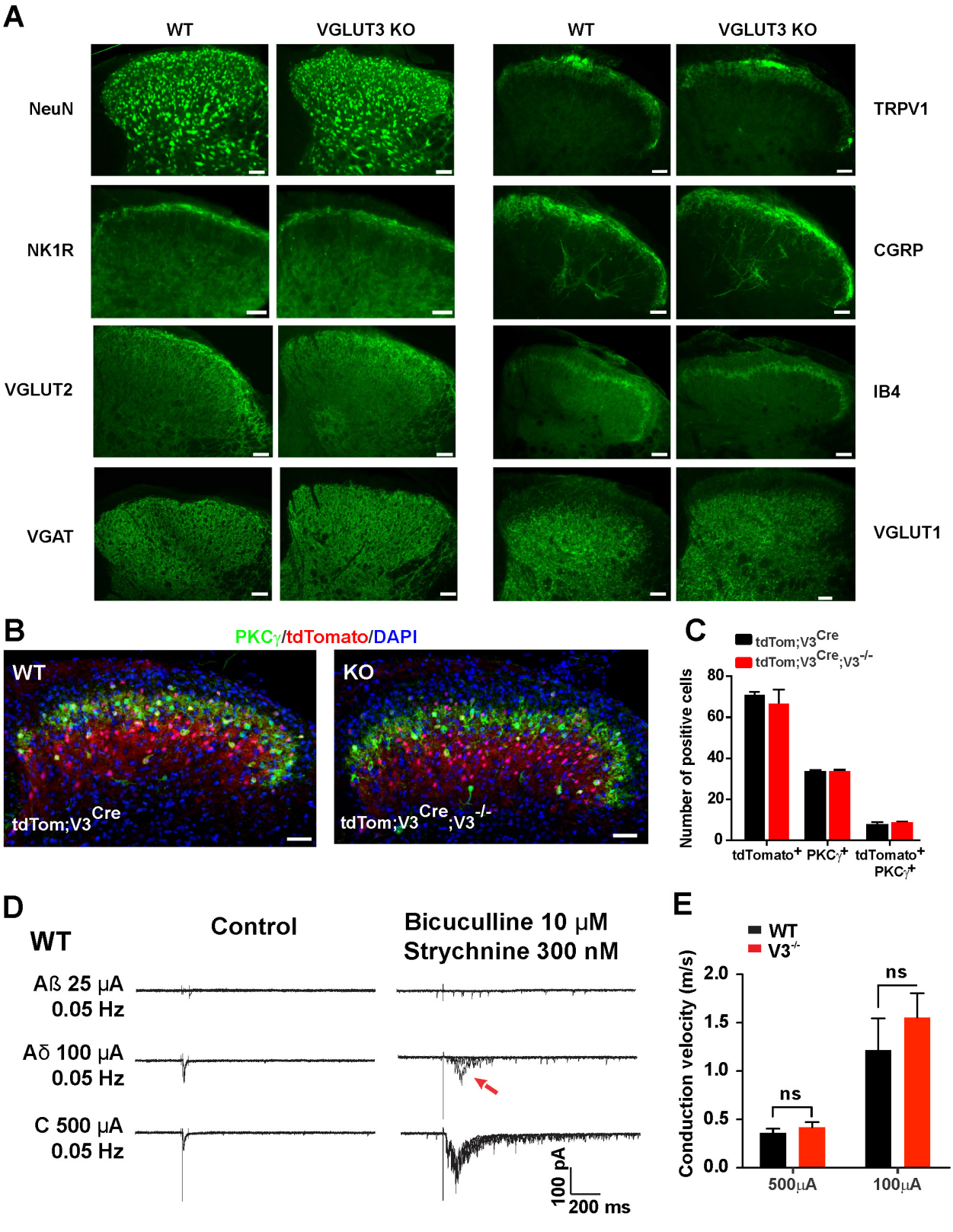
A
WT
VGLUT3 KO
WT
VGLUT3 KO
NeuN
TRPV1
NK1R
CGRP
VGLUT2
IB4
VGAT
VGLUT1
B
PKCγ/tdTomato/DAPI
WT
tdTom;V3Cre
KO
tdTom;V3Cre;V3-/-
C
tdTom;V3Cre
tdTom;V3Cre;V3-/-
Number of positive cells
80
60
40
20
0
tdTomato+
PKCγ+
tdTomato+ PKCγ+
D
WT
Control
Bicuculline 10 μM
Strychnine 300 nM
Aß 25 μA
0.05 Hz
Aδ 100 μA
0.05 Hz
C 500 μA
0.05 Hz
100 pA
200 ms
E
WT
V3-/-
Conduction velocity (m/s)
2.0
1.5
1.0
0.5
0.0
ns
ns
500μA
100μA

Figure S2, Related to Figure 4. Architecture, afferent innervation and afferent electrophysiology are normal in VGLUT3 KO dorsal horn.

(A) Spinal cords of VGLUT3 KO and WT mice stained for markers of spinal cord neurons (NeuN, VGLUT2, VGAT, NK1) and primary afferents (IB4, CGRP, TRPV1, VGLUT1) show no gross differences. Scale bars = 100 μm.

(B) Dorsal horns of lsl-tdTom;VGLUT3^{Cre} mice on a VGLUT3 KO or WT background are co-stained with PKCγ and DAPI. Scale bars = 20 μm.

(C) The number of tomato^{+} and PKCγ^{+} cells in the dorsal horn of lsl-tdTom;VGLUT3^{Cre} mice does not differ in the absence of VGLUT3.

(D) Example of polysynaptic EPSCs (red arrow) induced by stimulation of Aβ and Aδ fibers (100 μA) under pharmacological disinhibition.

(E) Conduction velocities and primary afferent thresholds are similar between VGLUT3 KO and WT (n = 7 and 8 respectively, Mann-Whitney test).

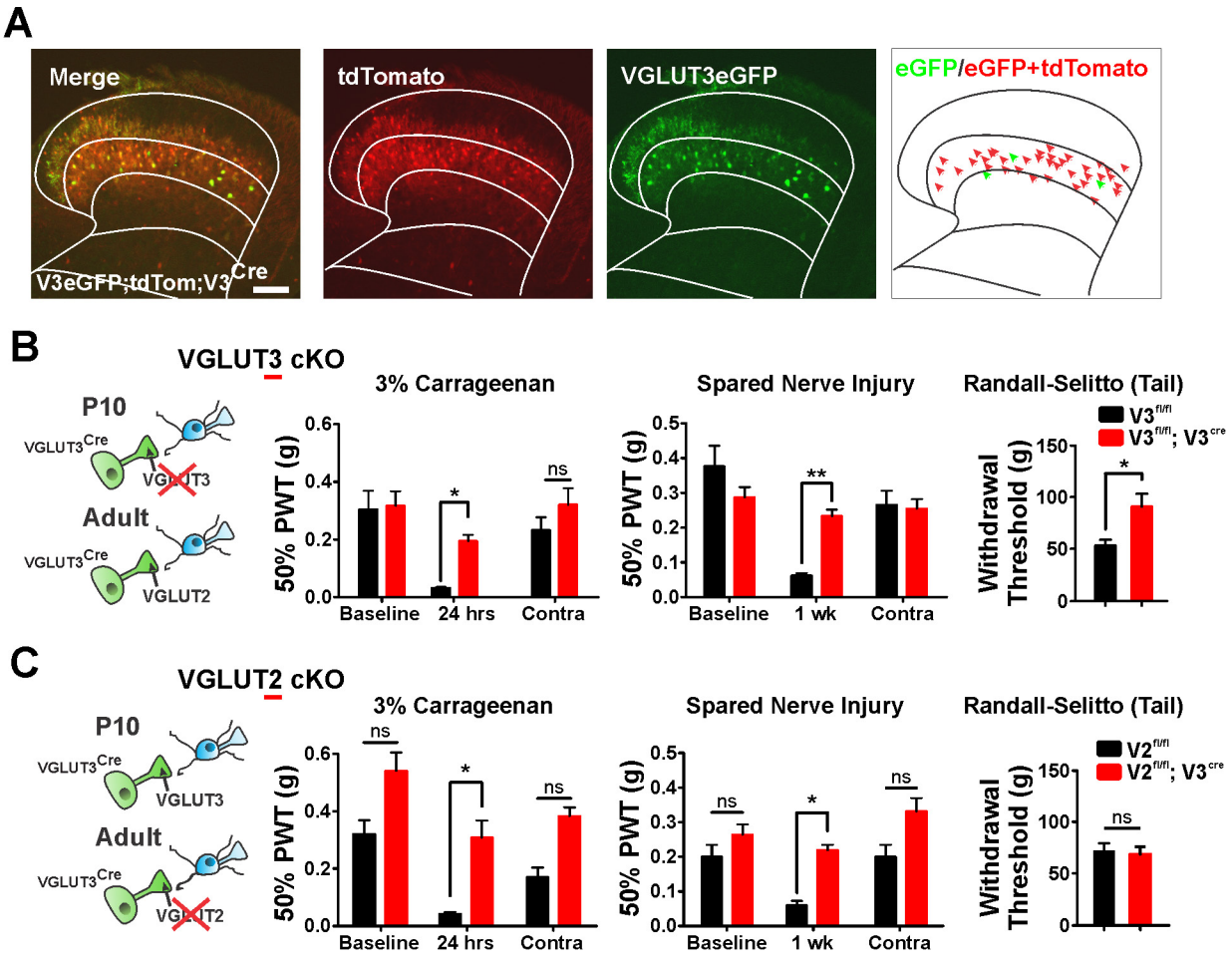

Figure S3, Related to Figure 5. Mechanical pain behavior after deletion of VGLUT2 or VGLUT3 in VGLUT3^{Cre} neurons.

(A) VGLUT3^{EGFP};lsl-tdTom;VGLUT3^{Cre} mice, EGFP co-localizes with tomato. Scale bar = 100 μm.

(B) VGLUT3$^{fl/fl}$; VGLUT3^{Cre} mice lack transient VGLUT3 expression in the dorsal horn. Baseline PWTs of VGLUT3$^{fl/fl}$;VGLUT3^{Cre} mice are similar to controls. After carrageenan or SNI, PWTs are significantly elevated compared to controls (both tests n=7 both groups). Randall-Selitto withdrawal thresholds are also significantly higher than controls (n=4 both groups).

(C) VGLUT2$^{fl/fl}$;VGLUT3^{Cre} mice lack adult VGLUT2 expression in VGLUT3 transient cells. Baseline PWTs of VGLUT2$^{fl/fl}$;VGLUT3^{Cre} mice are similar to controls. After carrageenan (n=5 both groups) or SNI (n=3 both groups), PWTs are significantly elevated compared to controls Remarkably, Randall-Selitto withdrawal thresholds of VGLUT2$^{fl/fl}$;VGLUT3^{Cre} do not differ from controls (n=4 both groups).

Data are Mean ± SEM. *$p < 0.05$, **$p \leq 0.01$.

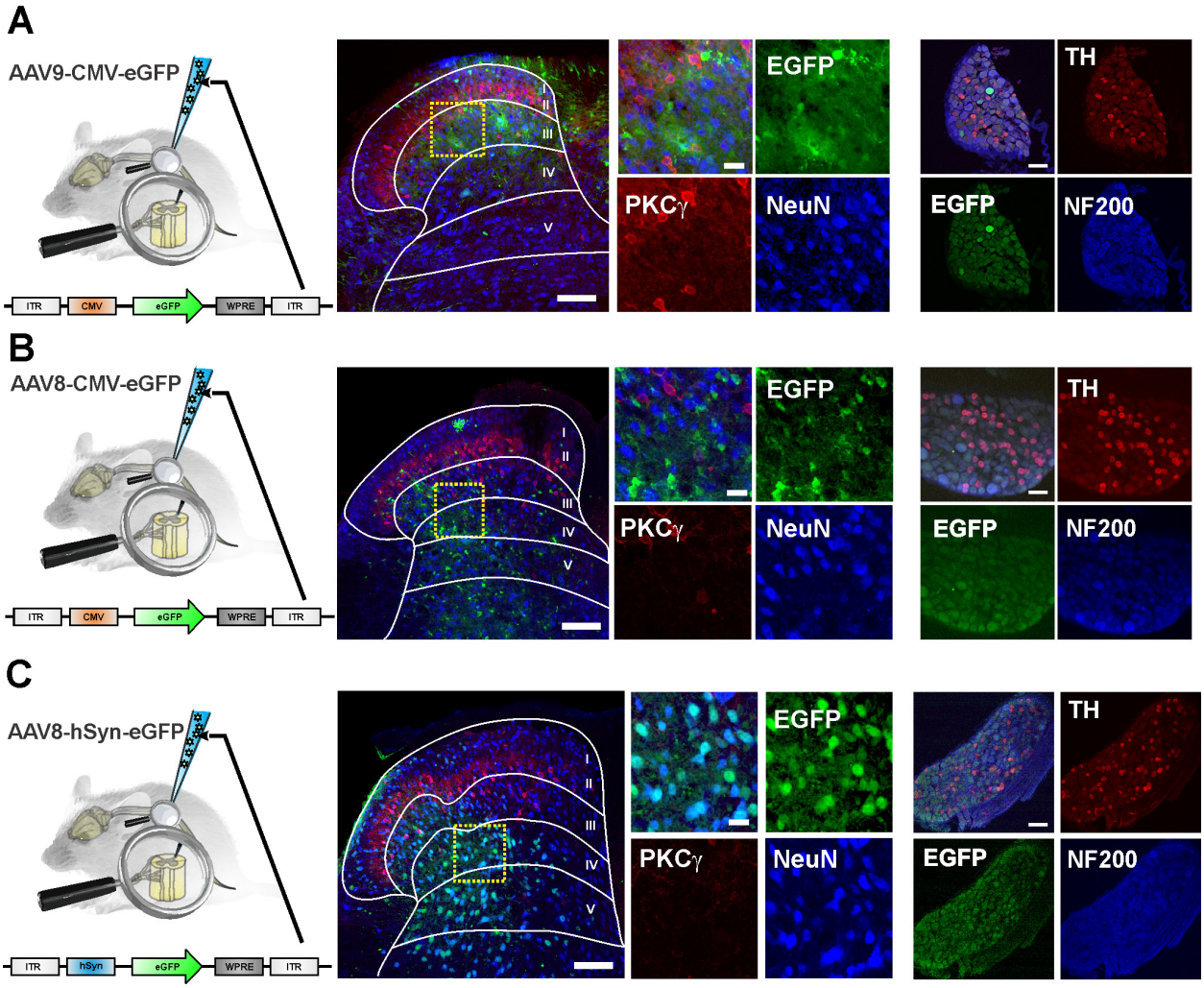

Figure S4, Related to Figure 5. Transduction of dorsal horn neurons and DRG with AAVs.

(A) AAV9-CMV-EGFP infects dorsal horn neurons and glia as well as DRG neurons. Scale bars = 100 μm except for inset (10 μm).

(B) AAV8-CMV-EGFP infects dorsal horn glia and some neurons, but not DRG. Scale bars = 100 μm except for inset (10 μm).

(C) AAV8-hSyn-EGFP exclusively infects dorsal horn neurons, not glia or DRG. Scale bars = 100 μm except for inset (10 μm).

MERGE
cFos
mCherry
NeuN
WT-DREADDs CNO-Mech
KO-DREADDs CNO-Mech
WT CNO-Mech
WT-DREADDs CNO
KO-DREADDs CNO
WT-DREADDs Saline
I
II
III
IV
V
V3Cre
V3fl/fl;V3Cre

Figure S5, Related to Figure 5. Induction of c-Fos in the dorsal horn by hM3Dq activation. Representative images of c-Fos induction in dorsal horn neurons of VGLUT3^{Cre} (labeled WT) or VGLUT3$^{fl/fl}$;VGLUT3^{Cre} (labeled KO) mice with and without injection of hM3Dq-mCherry virus, CNO or mechanical stimulation of the plantar hindpaw. All scale bars = 100 μm.

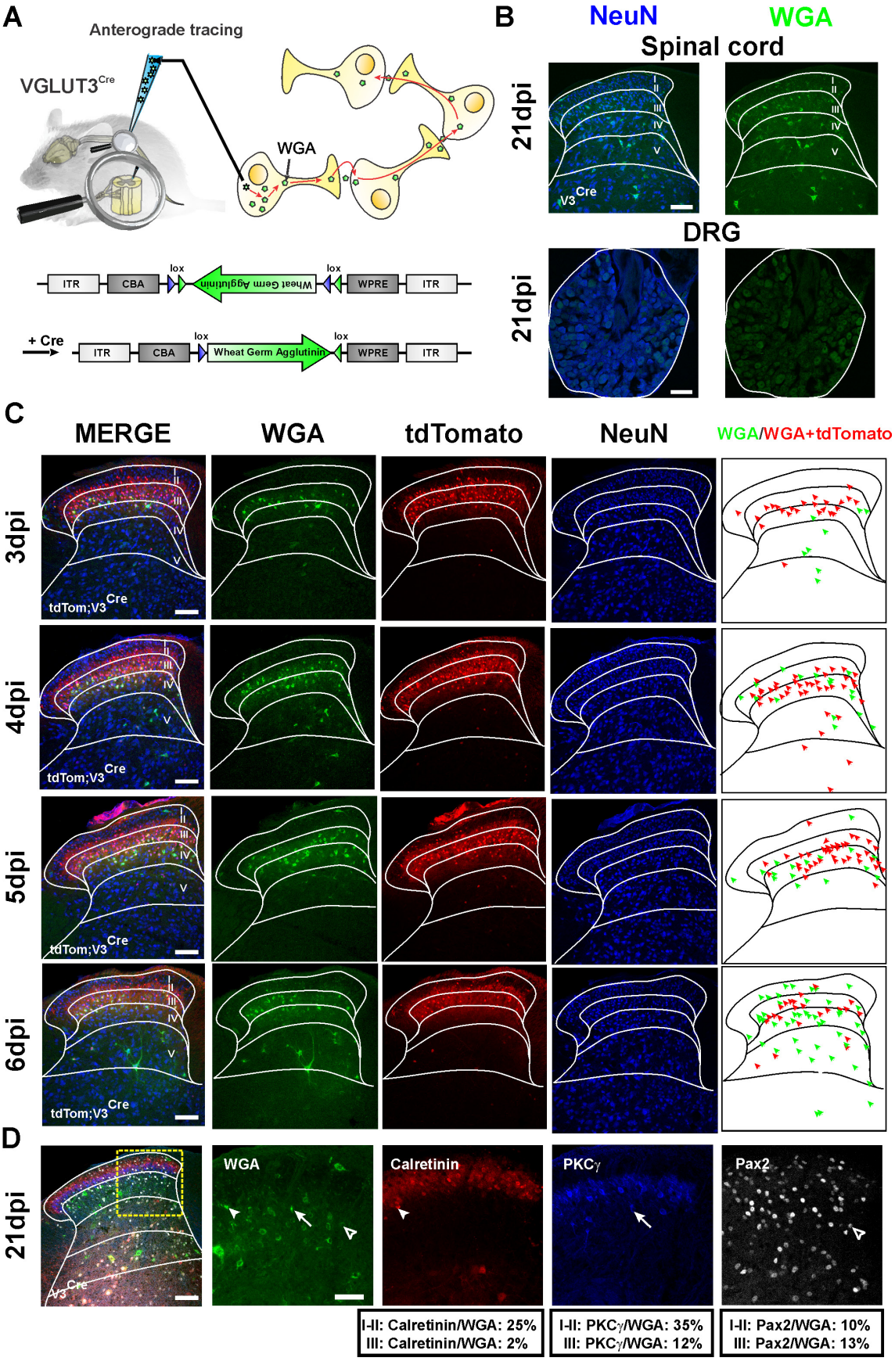
A
Anterograde tracing
VGLUT3Cre
WGA
ITR
CBA
lox
Wheat Germ Agglutinin
WPRE
+ Cre
B
NeuN
WGA
Spinal cord
21dpi
Cre
V3
DRG
C
MERGE
WGA
tdTomato
NeuN
WGA/WGA+tdTomato
3dpi
4dpi
5dpi
6dpi
tdTom;V3Cre
D
21dpi
Calretinin
PKCγ
Pax2
I-II: Calretinin/WGA: 25%
III: Calretinin/WGA: 2%
I-II: PKCγ/WGA: 35%
III: PKCγ/WGA: 12%
I-II: Pax2/WGA: 10%
III: Pax2/WGA: 13%

Figure S6, Related to Figure 5. Anterograde tracing with wheat germ agglutinin in lsl-tdTom;VGLUT3 mice.

(A) Schematic of lsl-tdTom;VGLUT3^{Cre} mice unilaterally injected with AAV2-CBA-Flex-WGA in the dorsal horn at p10.

(B) At 21 days post-injection (dpi), WGA is observed in all laminae of the dorsal horn but is not present in DRG neurons.

(C) From 3-6 dpi, WGA starts in tdTomato^{+} cells and then spreads to cells in laminae III and IV-V with time.

(D) At 21 dpi, WGA is observed in many more cells including calretinin (25%) and PKCγ (35%) excitatory interneurons and Pax2 (10%) inhibitory interneurons in lamina II. All scale bars = 100 μm except in D (50 μm).

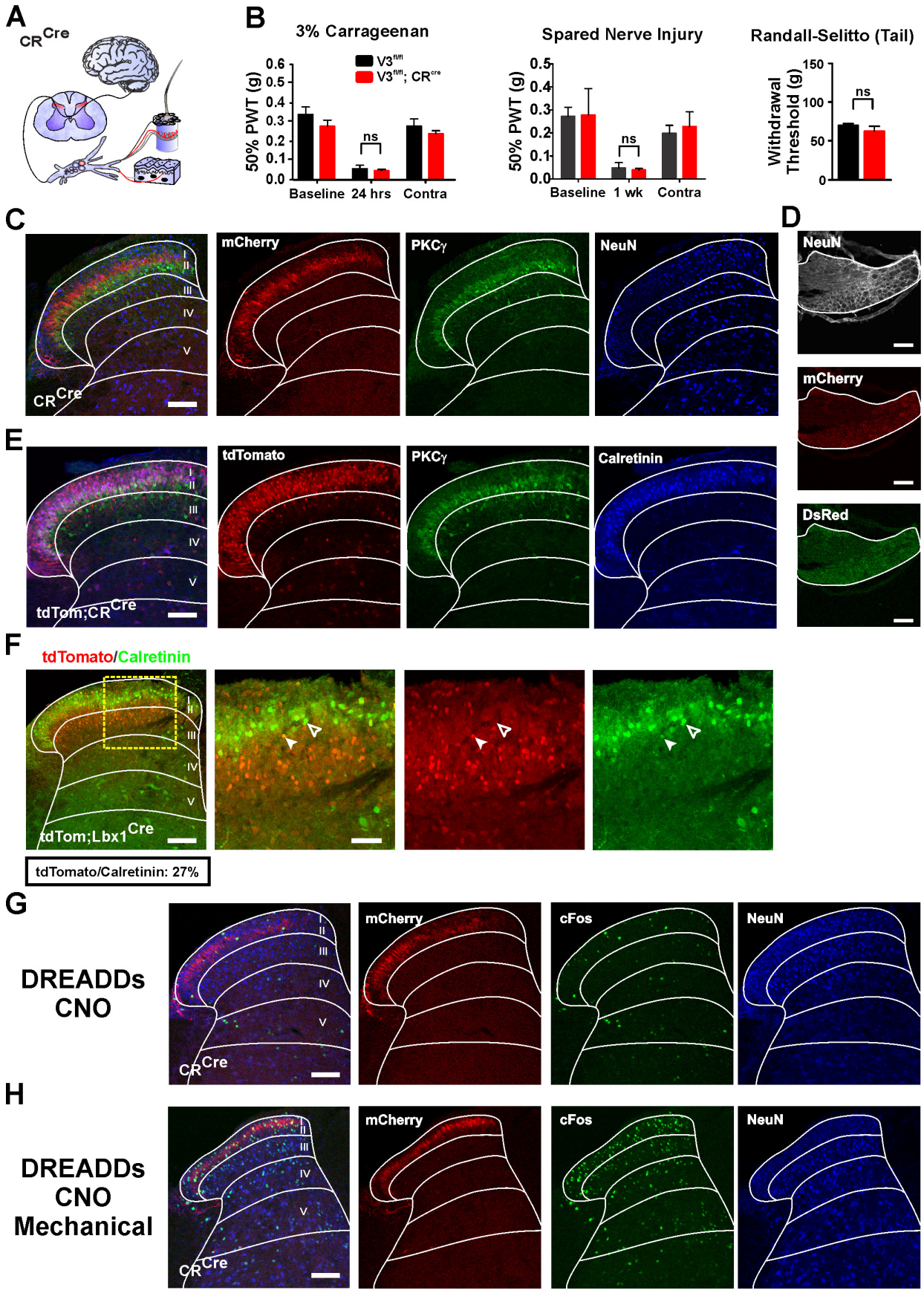
A
CR Cre
B
3% Carrageenan
V3 fl/fl
V3 fl/fl; CR cre
50% PWT (g)
0.6
0.5
0.4
0.3
0.2
0.1
0.0
ns
Baseline
24 hrs
Contra
Spared Nerve Injury
50% PWT (g)
0.5
0.4
0.3
0.2
0.1
0.0
ns
Baseline
1 wk
Contra
Randall-Selitto (Tail)
Withdrawal Threshold (g)
150
100
50
0
ns
C
I
II
III
IV
V
CR Cre
mCherry
PKCγ
NeuN
D
NeuN
mCherry
DsRed
E
tdTom;CR Cre
tdTomato
PKCγ
Calretinin
F
tdTomato/Calretinin
tdTom;Lbx1 Cre
tdTomato/Calretinin: 27%
G
DREADDs
CNO
CR Cre
mCherry
cFos
NeuN
H
DREADDs
CNO
Mechanical
CR Cre
mCherry
cFos
NeuN

Figure S7, Related to Figure 7. Behavioral characterization and cFos induction using CR^{Cre} Mice.

(A) In CR^{Cre} mice, dorsal horn excitatory neurons and some DRG neurons express Cre.

(B) Loss of VGLUT3 from calretinin neurons does not alter PWTs at baseline or after carrageenan (n=4 both groups) or SNI (n=2 both groups). Randall-Selitto thresholds are also unchanged (n=4 both groups).

(C) In CR^{Cre} mice injected unilaterally in the dorsal horn with AAV8-hSyn-DIO-hM3Dq-mCherry virus, mCherry localizes exclusively to the dorsal region of lamina II_i, and does not co-localize with PKCγ.

(D) In CR^{Cre} mice injected unilaterally in the dorsal horn with AAV8-hSyn-DIO-hM3Dq-mCherry virus, mCherry is not expressed by DRG.

(E) In lsl-tdTom;CR^{Cre} mice, tomato is expressed by neurons throughout lamina II_i and co-stains almost completely with calretinin, but very little with PKCγ.

(F) In adult lsl-tdTom;$Lbx1^{Cre}$, a few calretinin neurons in lamina II_i co-localize with tomato (closed arrowhead), but most do not (open arrowhead).

(G) Representative images of c-Fos induction in dorsal horn neurons of CR^{Cre} expressing hM3Dq-mCherry virus and injected with CNO.

(H) Representative images of c-Fos induction in dorsal horn neurons of CR^{Cre} expressing hM3Dq-mCherry virus and injected with CNO plus mechanical stimulation of the plantar hindpaw.

Data are Mean ± SEM. All scale bars = 100 μm except insets in F (20 μm).

Movie S1, Related to Figure 5. Spontaneous allodynia behavior after CNO administration in VGLUT3^{Cre} and VGLUT3$^{fl/fl}$;VGLUT3^{Cre} mice expressing hM3Dq-mCherry. After saline injection, VGLUT3^{Cre} mice expressing the hM3Dq receptor show no abnormal paw behaviors. After administration of 5 mg/kg CNO, VGLUT3^{Cre} mice show paw lifting (first arrow) and paw guarding behaviors (second and third arrow). VGLUT3$^{fl/fl}$;VGLUT3^{Cre} mice show very subdued paw lifting and guarding behavior after CNO injection (arrow).

Movie S2, Related to Figure 7. Spontaneous allodynia behavior after CNO administration in CR^{Cre} mice expressing hM3Dq-mCherry. After saline injection, CR^{Cre} mice expressing the hM3Dq receptor show no abnormal paw behaviors. After administration of 5 mg/kg CNO, CR^{Cre} mice show paw lifting and paw guarding behaviors (arrow).

SUPPLEMENTAL EXPERIMENTAL PROCEDURES

Animals

All mice were kept on a standard 12:12 light/dark cycle in micro-isolator caging racks (Allentown Caging) with food and water provided *ad libitum* and were treated in accordance with protocols approved by the Institutional Animal Care and Use Committee at the University of Pittsburgh and UCSF. $Rosa26^{lsl\text{-}td}$ (stock #007914), $Rosa26^{Cre}$ (stock #006054), $Rosa26^{Flpe}$ (stock #003946), CR^{Cre} (stock #010774) and $KRT14^{Cre}$ (stock #004782) mouse lines were obtained from Jackson Laboratories. Dr. Rohini Kuner provided the SNS^{Cre} mice, Dr. Fan Wang provided the $Advillin^{Cre}$ mice, Dr. Hanns-Uli Zeilhofer provided the $Hoxb8^{Cre}$ mice, Dr. Qiufu Ma provided $Tlx3^{Cre}$ mice, Dr. Carmen Birchmeier provided the $Lbx1^{Cre}$ mice and Dr. Thomas Hnasko provided the $VGLUT2^{fl/fl}$ mice.

Description of Conditional VGLUT3 knockout mouse. The mouse was generated by homologous recombination in embryonic stem (ES) cells. LoxP sites surround exon 2 in the targeting construct, which was generated from an RPCI-24 BAC clone. *Neomyocin* and *diphtheria toxin A* gene cassettes were used as positive and negative selectable markers. The targeting construct was introduced into 129/Ola ES cells. Properly targeted clones were injected into pseudopregnant C57Bl/6J mice. Chimeric founders were crossed to $Rosa26^{Flpe}$ to remove the *neomycin* gene. Germline deleted mice were generated by first crossing to $Rosa26^{Cre}$ ($VGLUT3^{\Delta/\Delta}$). Levels of VGLUT3 were assessed by Western blot of brain homogenate and immunofluorescence staining of spinal cord. VGLUT3 was present at WT levels in $VGLUT3^{fl/fl}$ mice and was absent from $VGLUT3^{\Delta/\Delta}$ mice.

Behavioral Tests

Randall-Selitto Assay

Mice were tested as previously reported (Seal et al., 2009). Briefly, mice were acclimated to a tail access restraint (StoeltingCo cat# 51338) by placing the open restraint in the home cage for 2 days prior to testing. On test day, mice were allowed to acclimate for 10 minutes to the restraint and then placed on the Ugo Basile Analgesy Meter (cat# 37215) with a blunt conical tip on the weight arm. Force was applied to the tail until the mouse struggled or flicked its tail (withdrawal threshold). The final force in grams was recorded. Each mouse was tested 3 times with a ten-minute inter-trial interval and the results of the three trials averaged.

Paw Withdrawal Threshold to von Frey Filaments

Mice were tested as previously described (Seal et al., 2009). Briefly, mice were habituated to opaque Plexiglas chambers on a wire mesh table for 1 hour the day before and 30 minutes prior to testing. Testing was performed using a set of calibrated Semmes-Weinstein monofilaments (StoeltingCo cat# 58011) using the Up-Down method (Chaplan et al., 1994). The 50% paw withdraw threshold (PWT) was determined for each mouse beginning with a 0.4 g filament. Each filament was applied to the plantar surface of the hind paw between the walking pads for 3 seconds or until a response such as a sharp withdrawal, shaking or licking of the limb was observed. Incidents of rearing or normal ambulation during filament application were not counted. Testing alternated between the ipsilateral and contralateral paws with a 5-minute interval in between each application until the thresholds were determined.

Pinprick test

Animals were first placed in a square Plexiglas chamber on top of a wire mesh table. Animals were acclimated to this testing arena for 1 hour on the day prior to testing and for an additional 30 minutes immediately before testing. A small insect pin (tip diameter = 0.03 mm) was applied with minimal pressure to the plantar surface of the left hind paw, taking care not to penetrate the skin. If the animal showed aversive behavior (lifting, shaking, licking of the paw) a positive response was recorded. A negative response was recorded if the animal showed no such reaction within 2 seconds of application. The application was repeated 10 times with a 5-minute interval between applications, and a percentage positive response determined for each animal.

Fur Clip Test

Animals were placed in an empty plastic chamber and allowed to acclimate for 15-20 minutes. A 2 cm wide alligator clip was attached to the hairs on the animal's back just above the tail, taking care not to pinch the skin. The latency (in seconds) until the animal looked towards the clip or tried to remove it was recorded. Three applications were performed per animal with a five-minute interval between applications, and the average response latency determined for each animal out of three trials.

Sticky Tape Test

Animals were placed in an empty plastic chamber and allowed to acclimate for 15-20 minutes. A ¼ inch diameter adhesive paper circle was then applied to the plantar surface of the left hind paw covering the footpads, and the animals were placed back in the cage. The latency until each animal responded to the sticky tape (by licking, looking

at or shaking of the affected paw) was then recorded and the tape circle removed. Each animal was tested 3 times with a 5-mintute interval between tests, and the three values averaged for each animal.

Dynamic Mechanical Allodynia (Cotton Swab Method)

The test was performed as described previously (Garrison and Stucky 2011). Briefly, animals were first placed in a square Plexiglas chamber on top of a wire mesh table and allowed to acclimate to this testing arena for 1 hour prior to testing. Using forceps, the head of a cotton swab was teased and puffed out until it reached approximately three times its original size. The cotton swab was lightly run across the surface of the hind paw from heel to toe. If the animal reacted (lifting, shaking, licking of the paw) a positive response was recorded. A negative response was recorded if the animal showed no such behavior. The application was repeated 10 times with a 5-minute interval between applications, and a percentage positive response determined for each animal.

Plantar Heat Test (Hargreaves' Method)

Animals were placed in a acrylic chamber on a glass top table and allowed to acclimate to the test chamber for 1 hour the day before and 30 minutes the day of testing. Using a Plantar Analgesia Meter (IITC) a radiant heat source of constant intensity was focused on the plantar surface of the hindpaw and the latency to paw withdrawal measured. The heat source was shut off upon paw withdrawal or after 20 seconds of exposure to prevent injury. The test was repeated 3 times on each hind paw with a 5 minute interval between tests and the results for each paw averaged together.

Carrageenan-induced inflammation

Mice were lightly anesthetized via inhaled 2.5% isoflurane and injected with 20 µL of 3% λ-Carrageenan (Sigma 22049) dissolved in sterile 0.9% NaCl into the plantar surface of the left hind paw. PWTs were determined before and 24 hours after injection.

Spared Nerve Injury

Surgery was performed as previously described (Seal et al., 2009; Shields et al., 2003). Briefly, Mice were deeply anesthetized using a mix of 100 mg/kg ketamine and 20 mg/kg xylazine by intraperitoneal injection. The left hind limb was shaved with trimmers and sterilized with betadine and ethanol. A small incision was made in the skin of the leg proximal to the knee and the skin and underlying muscle opened by blunt dissection to expose the three branches of the sciatic nerve. The peroneal and sural branches were tightly ligated with 6-0 nylon sutures and transected below the ligature, and a 2-3 mm section distal to the ligature was removed. Care was taken to avoid disturbing the tibial nerve, which was left intact. The muscle tissue was closed back over the nerves and the skin sutured shut with 6-0 nylon sutures. PWT to von Frey filaments were determined the day before and 1 week after surgery.

Chemogenetic Activation of hM3Dq Receptor

Von Frey and Hargreaves thresholds were performed as described above in AAV8-hSyn-DIO-hM3Dq-mCherry injected mice. Clozapine-N-Oxide (CNO) at 5 mg/kg was injected intraperitoneally 30 minutes prior to testing.

Paw Lifting/Guarding Assays

Mice were placed in a glass chamber with a smooth plastic floor and injected intraperitoneally with 5 mg/kg CNO in saline or saline only. The mouse was allowed to acclimate to the chamber for 15 minutes post-injection and then recorded by video for 10 minutes. The videos were then analyzed for incidents of the mouse visibly lifting or shaking its paw outside of ambulation (paw withdrawal), and time in which the paw was held such that the glabrous surface was not in contact with the floor or held in an abnormal posture tucked under the body (guarding).

Intraspinal AAV injections

P9-10 (for VGLUT3^{Cre}) or P15-16 (for CR^{Cre}) mice were anesthetized with 2.5% isoflurane. A midline incision along the left lumbar vertebrae was carefully performed until the spinal cord was visible from the intervertebral spaces. No laminectomy was performed to maximally avoid trauma. Glass microelectrode with around 50 µm tip was slowly inserted between L4-L5 at -250 µm from the dura using a stereotaxic frame avoiding the posterior spinal arteries. One µl of viral solution was slowly infused within a period of 5 minutes using a picospritzer and the micropipette was left in place for 2 minutes. The *lassimus dorsi* were sutured to protect the spinal cord and the skin was finally sealed with silk sutures. Animals were given an intraperitoneal injection of ketoprofen 5mg/kg before and 24h after the surgery. Behavior tests were performed 3 weeks after viral inoculation to allow maximal and stable expression. AAV8-CMV-eGFP (1.5 x 10^12 vg/ml), AAV9-CMV-eGFP (8 x 10^12 vg/ml), AAV8-hSyn-eGFP (3.7 x

10^12 vg/ml) and AAV8-hSyn-DiO-hM3Dq-mCherry (6 x 10^12 vg/ml) were purchased from UNC vector core (Chapel Hill, NC). AAV2-CBA-Flex-WGA (6.5 x 10^12 vg/ml) was a gift from Dr. Reza Sharif-Naeini.

Tissue processing for c-Fos analysis

For mice injected with the hM3Dq virus, animals were analyzed 3-5 weeks after viral injection. To investigate the expression of c-Fos after CNO in the absence of any other stimulus, animals were first anesthetized with an intraperitoneal injection of 1.5 g/kg urethane. After 30 minutes, control of proper anesthesia was assessed by the absence of reflex following a light pinch of the front paws. Then, mice were given an intraperitoneal injection of 3 mg/kg CNO or control saline and immediately placed on their back on a heating pad. Special care was taken to assure that the rear legs were not in contact to anything including the heating pad. 90 minutes after CNO injection, animals were quickly perfused as described below.

To investigate the effect of mechanical stimulation of the hindpaws following CNO injection, we used a rodent treadmill (Digigait, Mouse Specifics Inc.) as an unavoidable mechanical stimulus of the foot. To do so, mice were first placed into a Plexiglas chamber on the stationary treadmill and allowed to acclimate for 5 minutes. The speed was then slowly increased to a final rate of 10 cm/s for which lasted for a period of 5 minutes. At this final speed, animals were forced to walk but they never ran. At the end of this habituation period, mice were given an intraperitoneal injection of 3 mg/kg CNO. Animals were placed back into the chamber with the treadmill immobile and monitored for 30 minutes. The mice were then walked on the treadmill at a speed of

10 cm/s for a period of 15 minutes and finally placed back into their cage. While some mice showed discomfort, none failed to perform the task. Mice were perfused 90 minutes later as described below.

To investigate the effect of mechanical stimulation of the hindpaws following inflammation or neuropathy, mice were walked 24 hours after carrageenan injection or 1 week after SNI surgery respectively, and then perfused 90 minutes later as described above. Control mice that were not mechanically stimulated were taken from their home cages and immediately perfused.

Immunohistochemistry

Mice were deeply anesthetized with a mix of ketamine and xylazine and then transcardially perfused with phosphate-buffered saline (PBS) followed by 4% paraformaldehyde (PFA). A laminectomy was performed and the spinal cord and dorsal root ganglia harvested. Glabrous skin from the plantar surface of the hind paw was also removed. Tissues were post-fixed in 4% PFA overnight, cryo-protected in 30% sucrose and then cut with a cryostat (Microm HM550) into 10-30 µm sections placed directly onto poly-lysine coated slides or into wells containing PBS. For fluorescent immunostaining, spinal cord slices were blocked with 5% normal donkey serum (NDS) in PBS + 1% triton-X (PBS-T) for 1 hour at room temperature (RT) then incubated in primary antibody diluted in 5% NDS in PBS-T overnight at 4°C. Sections were then washed in PBS and incubated in AlexaFluor secondary antibodies (Jackson ImmunoResearch) diluted 1:1000 in 1% NDS in PBS-T, for 1-2 hours at RT. Slices were then washed in PBS and cover-slipped with Fluoromount-G or Fluoromount-G containing DAPI (Southern Biotech).

The following primary antibodies were used for immunofluorescence staining at the following dilutions: VGLUT3 antiserum raised in guinea pig (1:500; Synaptic Systems 135204), anti-PKCγ raised in rabbit (1:1000; Santa Cruz sc-211), anti-PKCγ raised in guinea pig (1:500; Frontier Institute Af350), anti-VGLUT1 raised in guinea pig (1:5000; Chemicon AB5905), anti-VGLUT2 raised in rabbit (1:1000; Synaptic Systems 135403), anti-tyrosine hydroxylase raised in rabbit (1:500; Chemicon AB152), anti-NF200 raised in mouse (1:1000; Sigma N0142), anti-TROMA1 raised in rat (1:50; University of Iowa DSHB), anti-CGRP raised in rabbit (1:1000; Penninsula Labs 4032), anti-TRPV1 raised in rabbit (1:1000; Alomone ACC-030), anti-NK1r raised in rabbit (1:2500; Sigma SAB4502913) anti-calretinin raised in mouse (1:1000; Swant 6B3), anti-Calbindin D-28K raised in mouse (1:1000; Swant 300), anti-Pax2 raised in Goat (1:200; R&D Systems AF3364), anti-c-Fos raised in rabbit (1:10,000; Millipore PC-38), anti-lectin (WGA) raised in rabbit (1:50,000; Sigma T4144), anti-EGFP raised in rabbit (1:1000, Life Technologies A6455), anti-VGAT raised in rabbit (1:2000, Millipore AB5062), anti-DsRed raised in rabbit (1:1000, Clontech 632496) and anti-NeuN raised in mouse (1:1000; Chemicon MAB377). We also used Isolectin B4-conjugated to Alexa-488 (1:200; Life Technologies I21411).

In Situ Hybridization

Spinal cord tissue was dissected, quickly frozen in isopentane at -30°C and then cut into 30 μm cryostat sections onto slides. Slides were stored at -80°C. Two-color fluorescent *in situ* hybridization followed the protocol of Ishii *et al.* with slight modification (Ishii et al., 2004). Slices were placed in cold 4% PFA for 20 minutes, washed at RT in PBS, incubated in 0.3% H2O2 for 30 minutes at RT, washed in PBS

and then incubated with proteinase K (10 µg/ml) for 5 minutes at 37°C, washed with PBS, and then incubated in 4% PFA at RT for 10 minutes, washed in PBS and then de-acetylated for 10' at RT, washed and then dehydrated the samples in graded series of ethanol (60-100%). Slices were then incubated in prehybridization solution (50% formamide, 10 mM Tris pH8.0, yeast tRNA, 10% dextran sulfate, 1x Denhardt's solution, 600 mM NaCl, 0.25% SDS, 1 mM EDTA, pH 8.0) at 63°C for 30 minutes. Probes were diluted in hybridization solution (100-200 ng/ml), heated to 85°C for 5', and then added to slides. Slices were incubated overnight at 63°C. Slices were washed for 30 minutes at 63°C in 2x standard saline citrate (SSC) + 50% formamide and then incubated in RNase A in buffer at 37°C for 30 minutes. Slices were then washed in a series of decreasing concentrations of SSC (2x, 0.2x, 0.1x) for 20 minutes at 65°C, blocked with Roche blocking buffer (0.5%) for 1 hour and then incubated with sheep anti-dig-AP (Roche) and rabbit anti-flu-POD (Roche) antibodies diluted in blocking buffer overnight at 4°C. Slides were washed with Tris-tween buffer and then incubated in with ABC tyramide solution (Perkin Elmer) for 10 minutes, washed and then incubated with streptavidin-conjugated to Alexa-488 at RT for one hour and incubated with HNPP/Fast Red (Roche) for 30 minutes. Slides were washed and cover-slipped with Fluoromount-G.

Fragments of genes encoding CCK, tomato, VGLUT2 and GAD67 were amplified by PCR from brain cDNA using primers taken from the Allan Brain Atlas. Each was subcloned into pBSK or pCRII (Invitrogen) and sequenced. Plasmids were linearized prior to probe synthesis. Probes were synthesized using DIG and Flu labeling kits (Roche).

Cell counting

Spinal cord sections were imaged with a Nikon A1R confocal laser-scanning microscope and Nikon Elements software using 405-, 488-, 561- and 640 nm excitation laser light. In order to suppress emission crosstalk, the microscope was configured to perform all scanning in sequential mode. Z-series were scanned at 20x magnification with an oil immersion lens and a z-step of 0.89 µm. Cells positive for tomato and/or PKCγ were scanned from three independent slices and averaged for each mouse (n = 3 per group). For cell counting, a 400 x 250 µm window was positioned so that its medial axis was perpendicular to the dorsal horn border with its medial end at the border between white and grey matter. Immunoreactive profiles were counted separately using the Fiji ImageJ 1.47 program (http://rsbweb.nih.gov/ij) cell counter plug-in. A cell was counted as immunopositive if (1) immunostaining of a single cell was clearly defined, (2) its level was at least two times that of the background levels, and (3) it had disappeared at both the top and bottom surfaces of z-stack as previously described (Peirs et al., 2014).

For c-Fos analysis, 5 slices from 1-3 animals with the highest viral expression were imaged with a z-step of 5 µm by an experimenter blind to the respective animal group. Lamina boundaries were traced based on Rexed lamination visible by NeuN staining using Fiji-ImageJ. Each image was then analyzed using only the channel corresponding to the c-Fos staining. Acquisition and analysis parameters were strictly identical during the entire experiment.

Electrophysiological recordings

Young-adult mice (P25 – P35) were deeply anesthetized with 100 mg/kg ketamine and 20 mg/kg xylazine. The spinal cord was quickly removed and transferred into an ice-cold (4°C) solution containing (in mM): 220 sucrose, 2.0 KCl, 7.0 MgCl2, 26 NaHCO3, 1.15 NaH2PO4, 11 D-glucose, and 0.5 CaCl2, (pH 7.4) bubbled with 95% O2 and 5% CO2. After removing the dura mater and ventral roots, the spinal cord was embedded into 3% low-melting agarose (Fisher Scientific BP165-25) and serial transverse slices (350 μm) were cut from the lumbar spinal cord with the dorsal roots and DRGS still attached using a vibroslice (Leica VT1000). Slices were incubated at 37^{o}C in an artificial cerebrospinal fluid (aCSF) containing (in mM): 118 NaCl, 3 KCl, 2.5 CaCl2, 1.5 MgSO4, 0.6 NaH2PO4, 25 NaHCO3, 10 glucose (290-300 mOsm), pH 7.4, bubbled with 95% O2 and 5% CO2, for a 60 min recovery period. For recordings of lamina I projection neurons, slices were incubated with aCSF containing 20 nM SP-TMR (SX 5800 Enzo Life Science) at room temperature for 20 min. After a 30 min period recovery, slices were transferred to a recording chamber (volume ≈1 ml) and held down with a pewter wire. The chamber was mounted on an upright microscope fitted with fluorescence optics (Carl Zeiss Axioskop 2) and linked to a Hamamatsu digital camera ORCA-R2. Slices were continuously perfused at 3.0 ml/min with the aCSF solution maintained at room temperature (≈ 25°C). Neurons were considered to be in lamina I within a 50 μm longitudinal area between the white matter border and the lamina II that has a distinct translucent appearance and can be easily distinguished under the microscope using a X10 objective lens. Positive fluorescent neurons were visualized using a X40 water-immersion objective lens and a Cy3 emission filter set under a 541-569 nm emission light delivered by a DG4 (Sutter Instruments) source.

Neurons were subsequently visualized using combined infrared and differential interference.

Patch pipettes were pulled from borosilicate glass tubing (Sutter Instrument) and filled with an internal solution containing (in mM): 135 K-gluconate, 4 NaCl, 2 MgCl2, 10 HEPES, 0.2 EGTA, 2.5 ATP-Na2, 0.5 GTP-Na, Dextran Alexa-488 (0.01%) (290 mOsm), pH 7.4. Pipette resistances ranged from 5–7 MΩ.

Whole-cell patch clamp recordings were acquired using an AxoPatch 200B amplifier and a Digidata 1440 digitizer (Axon laboratory) and pClamp 10.3 acquisition software. Voltage clamp data were low pass filtered at 5 kHz and digitized at 10 kHz. Junction potentials were corrected before gigaseal formation. Series resistance was monitored throughout the experiments and was not compensated. Data were discarded if series resistance varied more than ±20 MΩ. Voltage clamp data were recorded at a holding potential of -65 mV.

Dorsal roots were stimulated using a suction electrode at 25, 100 and 500 μA to activate Aβ or Aβ + Aδ or Aβ + Aδ + C fibers respectively at the low intensity of 0.05 Hz (duration 0.1 ms) using a A365 stimulus isolator (World Precision Instrument) as previously described (Torsney and MacDermott, 2006). At this intensity, both monosynaptic and polysynaptic EPSCs were observed. To address the monosynaptic nature of the response, the root was systematically stimulated five times at 0.05Hz, 1 Hz, 2Hz and 20 Hz. EPSCs were considered monosynaptic in an absence of synaptic failure or latency >2ms following a 20 Hz for Aβ fiber intensity stimulation, 2 Hz for Aδ fiber intensity stimulation and 1 Hz for C-fiber intensity stimulation as previously

described (Torsney and MacDermott, 2006). Conduction velocity was systematically measured for each root stimulation.

To address the effect of spinal disinhibition on evoked EPSCs recorded from lamina I $NK1^+$ neurons, 10 μM bicuculline and 300 nM strychnine were applied by perfusion application. Five minutes after spinal disinhibition, the root was stimulated and EPSCs recorded as described above.

To quantify the effect of spinal disinhibition on evoked EPSCs in lamina I $NK1^+$ neurons, area under the curve was measured from recordings in response to A-fiber stimulation at a 0.05 Hz frequency. Traces were filtered using a low pass Bessel filter at 1 kHz and polysynaptic EPSCs were quantified from the stimulation artifact to the end of the trace (≈ 20 s) from each trace and averaged. All data were analyzed offline using Clampfit 10.3 software (Axon instrument). Data are presented as the mean + SEM.

Neuronal morphology

Slice containing $VGLUT3^{Cre}$ neurons filled with 0.2% biocytin (Sigma Aldrich) for at least 20 minutes were used for neuron reconstruction. Tracer was revealed using Alexa488-conjugated streptavidin. Confocal images were taken with a 0.5 μm z-step and subsequently analyzed using Fiji-ImageJ. Single neurons were semi-automatically reconstructed using non-collapsed z-stacks imported in the simple neurite tracer plug-in as previously described (Alba-Delgado et al., 2015).

SUPPLEMENTAL REFERENCES

Alba-Delgado, C., El Khoueiry, C., Peirs, C., Dallel, R., Artola, A., and Antri, M. (2015). Subpopulations of PKCgamma interneurons within the medullary dorsal horn revealed by electrophysiological and morphological approach. Pain. Epub

Chaplan, S.R., Bach, F.W., Pogrel, J.W., Chung, J.M., and Yaksh, T.L. (1994). Quantitative assessment of tactile allodynia in the rat paw. J. Neurosci. Methods *53*, 55-63.

Garrison, S.R., Dietrich, A., Stucky, C.L. (2011). TRPC1 contributes to light-touch sensation and mechanical responses in low-threshold cutaneous sensory neurons. J. Neurophyiol. *107(3)*, 913-922.

Ishii, T., Omura, M., and Mombaerts, P. (2004). Protocols for two- and three-color fluorescent RNA in situ hybridization of the main and accessory olfactory epithelia in mouse. J. Neurocytol. *33*, 657-669.

Peirs, C., Patil, S., Bouali-Benazzouz, R., Artola, A., Landry, M., and Dallel, R. (2014). Protein kinase C gamma interneurons in the rat medullary dorsal horn: distribution and synaptic inputs to these neurons, and subcellular localization of the enzyme. J. Comp. Neurol. *522*, 393-413.

Seal, R.P., Wang, X., Guan, Y., Raja, S.N., Woodbury, C.J., Basbaum, A.I., and Edwards, R.H. (2009). Injury-induced mechanical hypersensitivity requires C-low threshold mechanoreceptors. Nature *462*, 651-655.

Shields, S.D., Eckert, W.A., 3rd, and Basbaum, A.I. (2003). Spared nerve injury model of neuropathic pain in the mouse: a behavioral and anatomic analysis. Pain *4*, 465-470.

Torsney, C., and MacDermott, A.B. (2006). Disinhibition opens the gate to pathological pain signaling in superficial neurokinin 1 receptor-expressing neurons in rat spinal cord. J. Neurosci. *26*, 1833-1843.